SAND2007-4059C

X-ray Imaging Diagnostics for HEDP and ICF Experiments

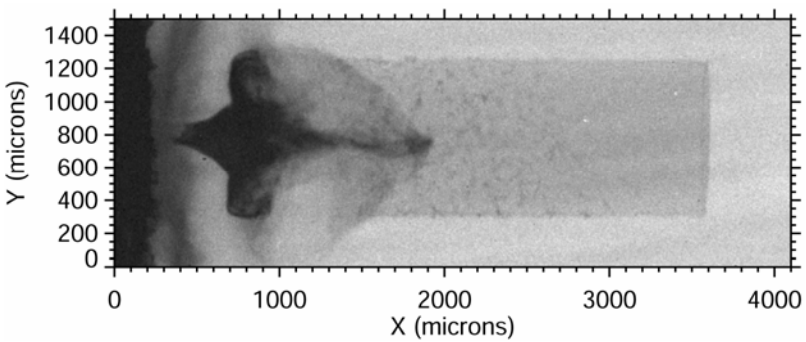

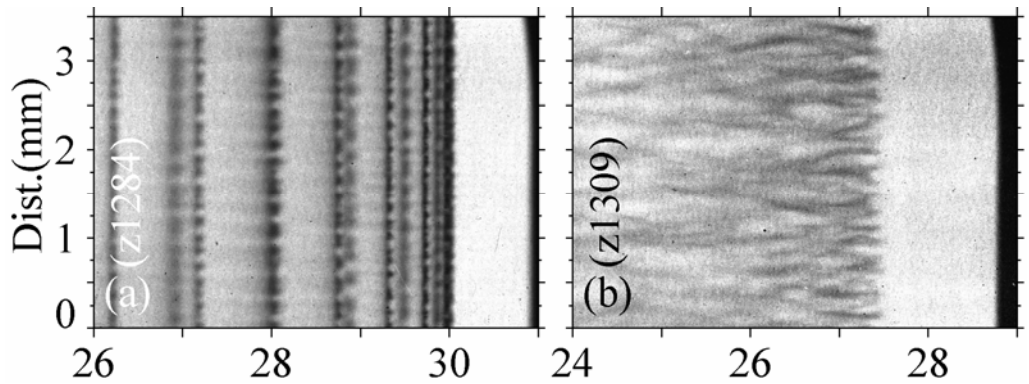

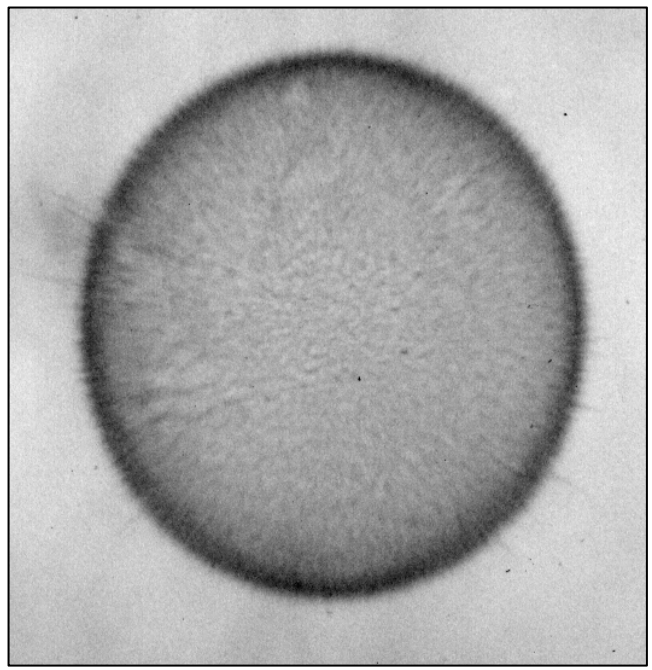

PPPS 2007 Minicourse

June 22, 2007

Daniel B. Sinars

Sandia National Laboratories

PO Box 5800, Albuquerque, NM 87185

Sandia is a multiprogram laboratory operated by Sandia Corporation, a Lockheed Martin Company, for the United States Department of Energy's National Nuclear Security Administration under contract DE-AC04-94AL85000.

NNSA National Nuclear Security Administration

Sandia National Laboratories

Table of Contents

Disclaimer: Example data and instrumentation biased toward z-pinch facilities due to author's experiences

Quick Review of X-ray Jargon

- 1 Å = "angstrom"
- 1 Å = 10^{-10} m = 0.1 nm
- 1 eV = "electron-volt"
- 1 eV = 1.602e-19 Joules (energy obtained by an electron accelerated across a 1 Volt potential)
- 1 keV = 1000 eV
- X-ray range is ~0.1-100 Å
- "Size" of hydrogen atom is about 0.5 Å, making x rays good probes of molecular/crystal structure

- Photon energies and wavelengths are related by quantum mechanics according to the following:

$$E = h\nu = \frac{hc}{\lambda}$$

$$E\,(eV) = 12{,}398 / \lambda\,(\text{Å})$$

The "x-ray" region is a broad range from ~0.1-100 keV (12.5 nm to 0.0125 nm)

0.1-10 keV X rays are particularly interesting for ICF and HEDP applications

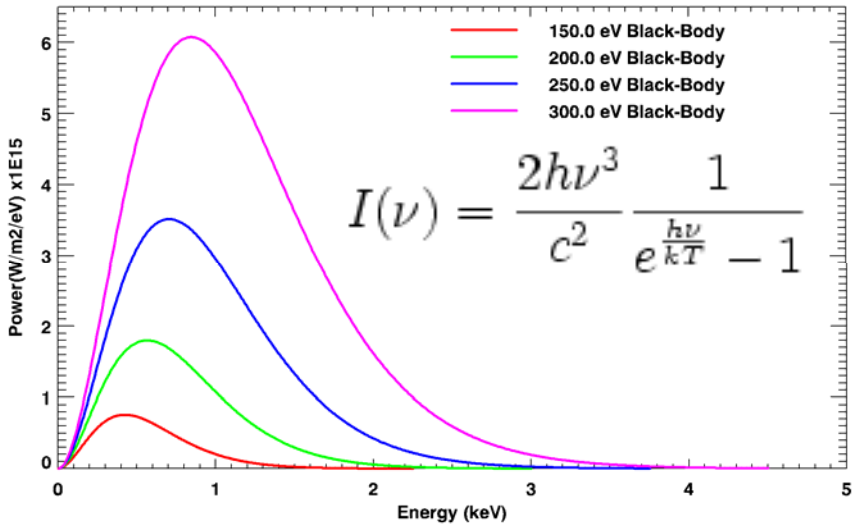

- The "x-ray" region spans a broad range from ~100 eV to ~100 keV (12.5 nm to 0.0125 nm)
- There is considerable interest in ~0.1-10 keV range for ICF/HEDP applications because the peak of typical achievable blackbody temperatures lies in this range.

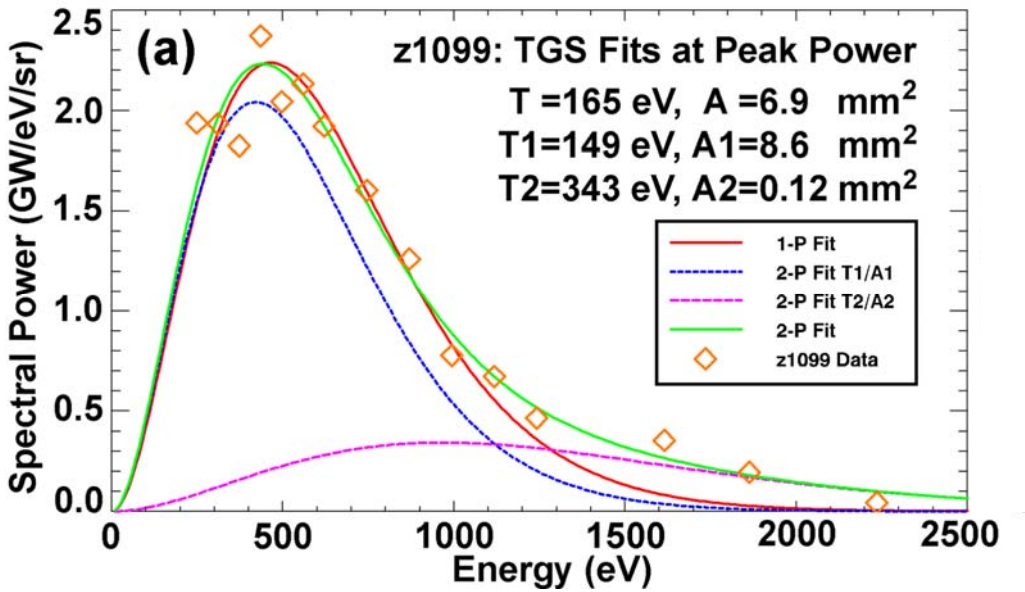

Example spectrum from a wire-array z-pinch

NIF hohlraums are expected to achieve ~280-300 eV

Sandia National Laboratories

Bremsstrahlung radiation can also be significant for some ICF/HEDP plasmas (e.g., z-pinches)

Bremsstrahlung radiation, or "braking radiation," comes from decelerating (or accelerating) electrons. It is also sometimes referred to as "free-free" radiation, because it refers to radiation from a free electron that interacts with another particle (e.g., an ion) but remains free after the interaction (i.e., it is not captured by the ion).

In a plasma, the electrons are continually producing bremsstrahlung from collisions with ions. The spectral power density is theoretically

$$\frac{dP_{Br}}{d\omega} = \frac{4\sqrt{2}}{3\sqrt{\pi}} \left[n_e r_e^3\right]^2 \left[\frac{m_e c^2}{T_e}\right]^{1/2} \left[\frac{m_e c^2}{r_e^3}\right] Z_{eff} E_1(w_m)$$

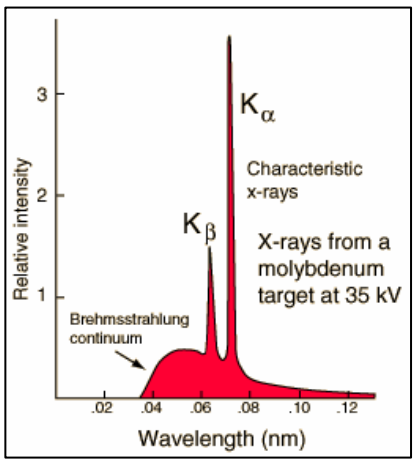

for a power density of

$$P_{Br} = \frac{8}{3} \left[n_e r_e^3\right]^2 \left[\frac{T_e}{m_e c^2}\right]^{1/2} \left[\frac{m_e c^3}{r_e^4}\right] Z_{eff} \alpha K$$

which in common units is

$$P_{Br}[\mathrm{Watt/m^3}] = \left[\frac{n_e}{7.69 \times 10^{18} \mathrm{m^{-3}}}\right]^2 T_e[\mathrm{eV}]^{1/2} Z_{eff}$$

NRL Plasma Formulary, 2006 Revision, p. 58.

Atoms and ions can produce x rays

- Electrons in atoms and ions live in “orbitals” with very specific energies
- If an incoming photon or electron transfers enough energy to a bound electron, it can “excite” the electron to an orbital with more energy
- Eventually an electron will de-excite from a higher orbital to a lower one, losing energy in the process and emitting a photon with that energy difference
- For most elements, these photons are in the x-ray range

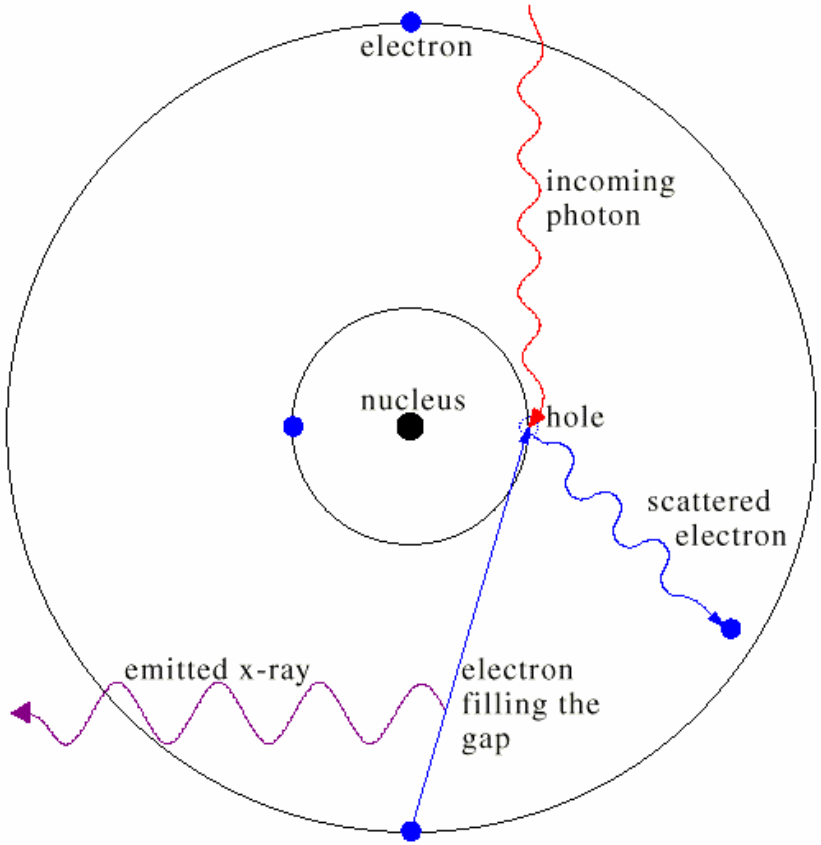

The electron orbital transitions result in x-ray photons with characteristic energies

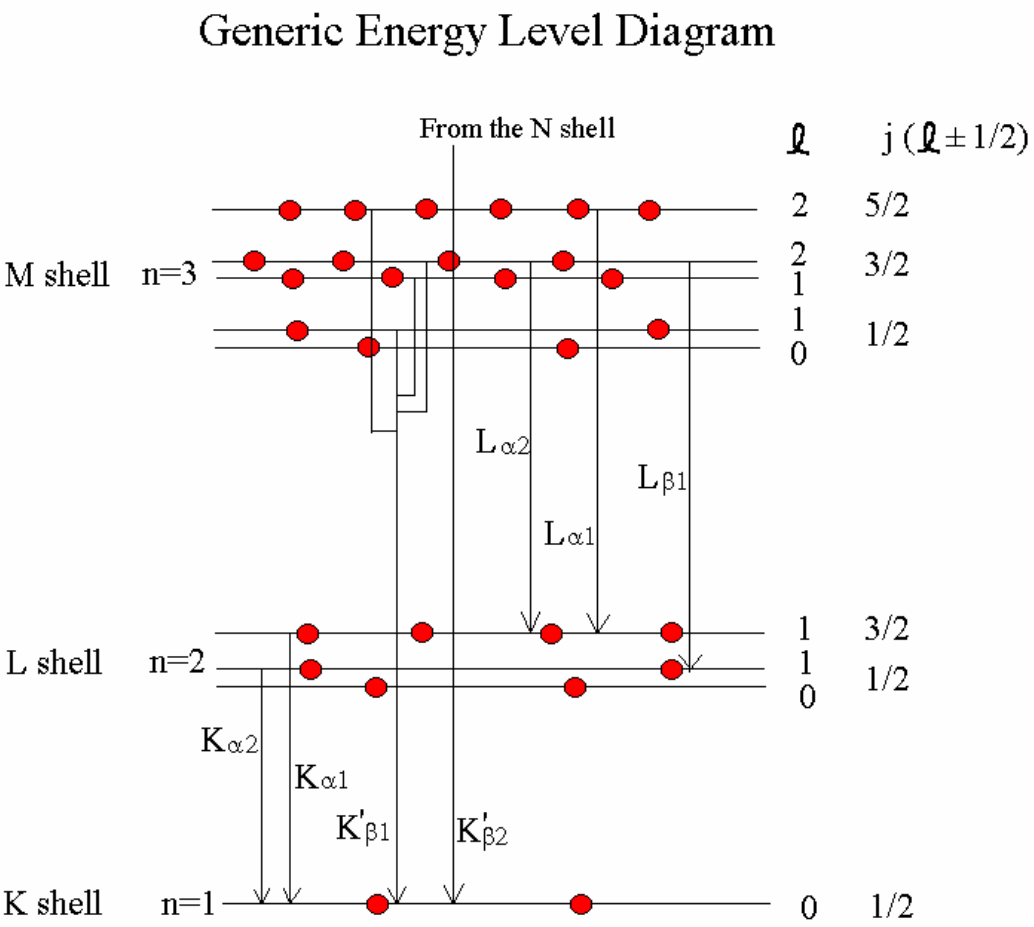

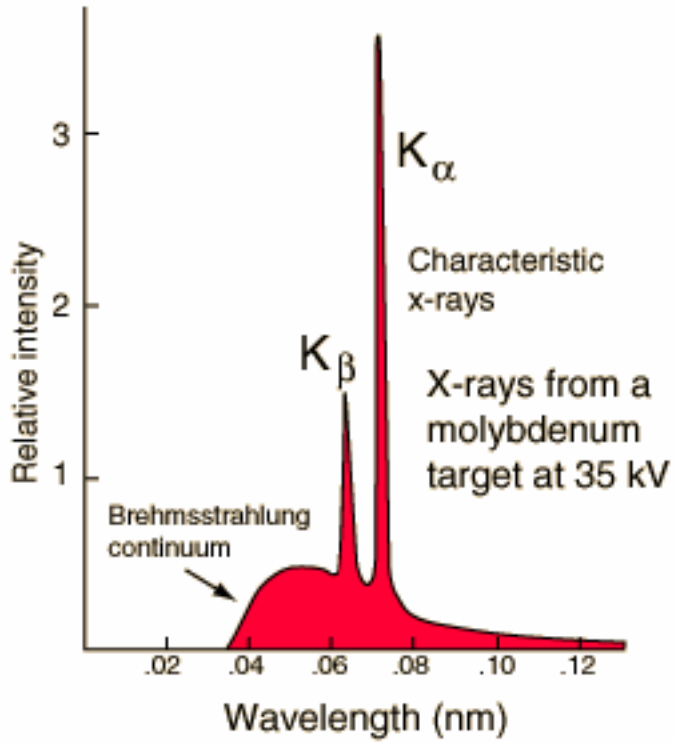

Each element emits “characteristic” x-ray lines that correspond to the electron transitions in the atom

Atomic transition energies predicted by Bohr Model

Sandia National Laboratories

Bohr's atomic model accurately predicts x-ray wavelengths

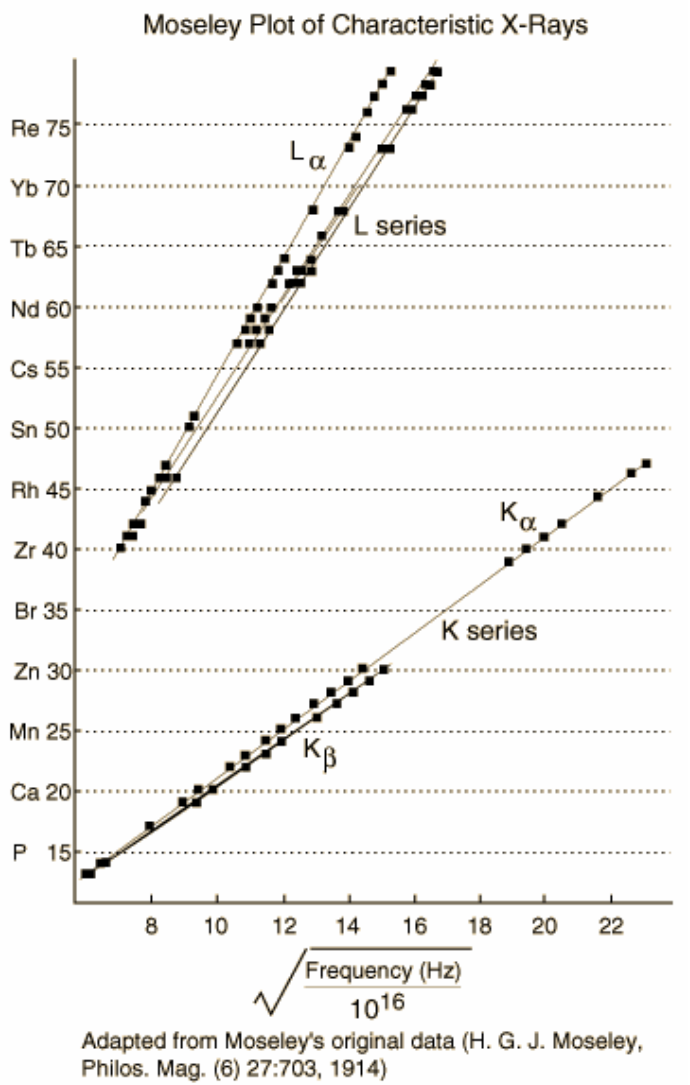

Adapted from Moseley's original data (H. G. J. Moseley, Philos. Mag. (6) 27:703, 1914)

Niels Bohr created a simple model that describes the energies of the electron orbitals in an atom

The Bohr Model for the Kα transitions:

$$h\upsilon_{K\alpha} = 13.6eV\ (Z-1)^2\left[\frac{1}{1^2}-\frac{1}{2^2}\right] = \frac{3}{4}13.6\,(Z-1)^2\ \ eV$$

This model predicts that the frequency (energy) of the emission varies with the square of the atomic number, a prediction verified by Henry Moseley in the diagram to the left.

Sandia National Laboratories

Lasers can be used to heat hohlraums to very high temperatures

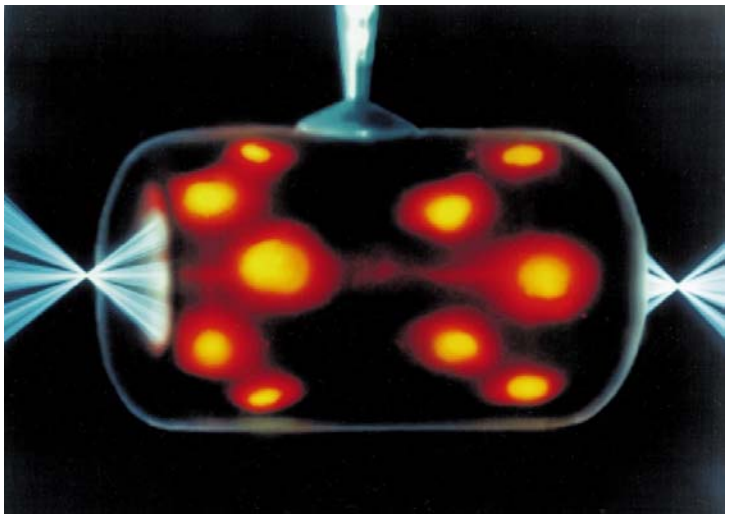

330 MJ stored
~1.8 MJ (~500 TW)
to target chamber

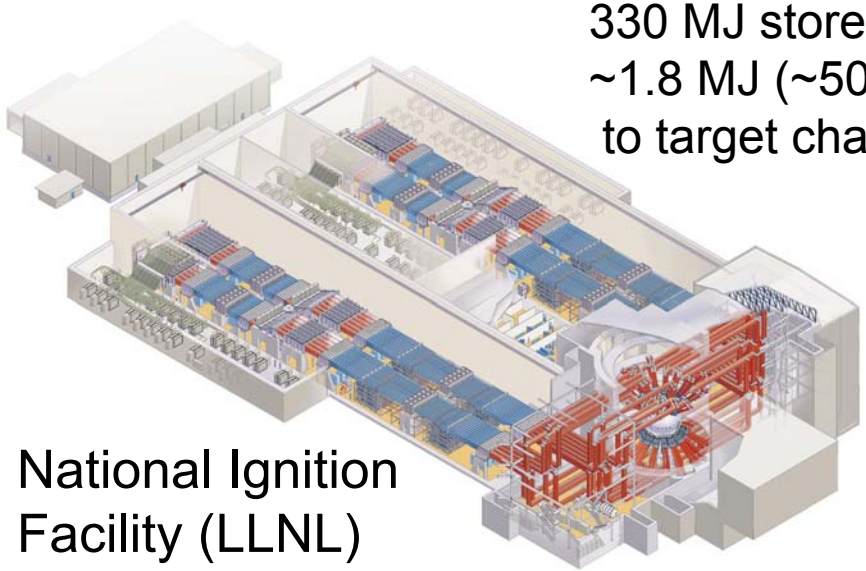

National Ignition Facility (LLNL)

Laser energy can be converted into thermal (blackbody) x-ray sources to drive inertial confinement fusion or HEDP experiments

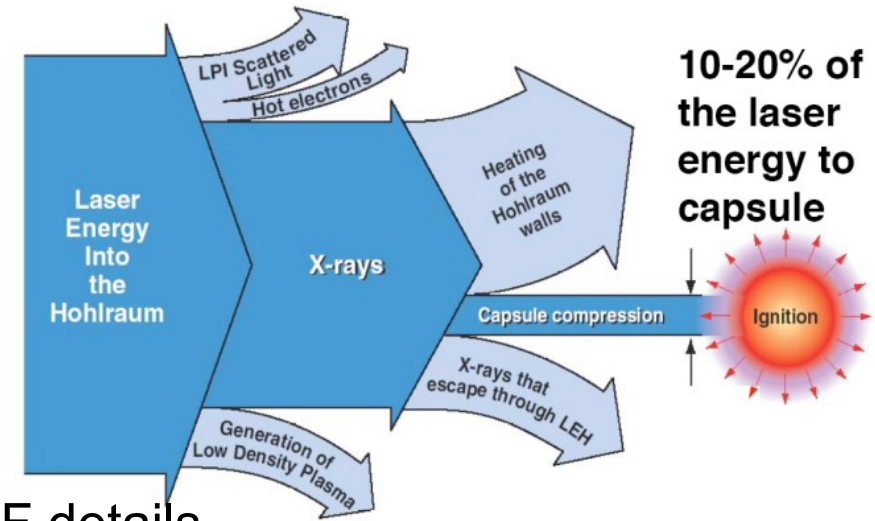

See Jeff Koch's presentation for better NIF details

Z-pinch plasmas can also be used to generate x rays for ICF/HEDP applications

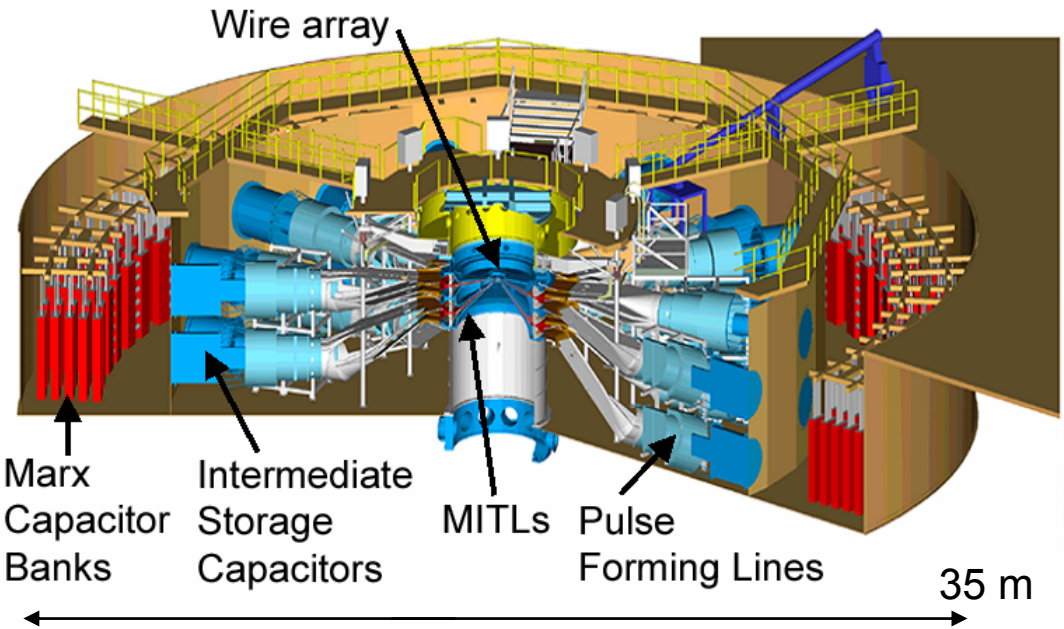

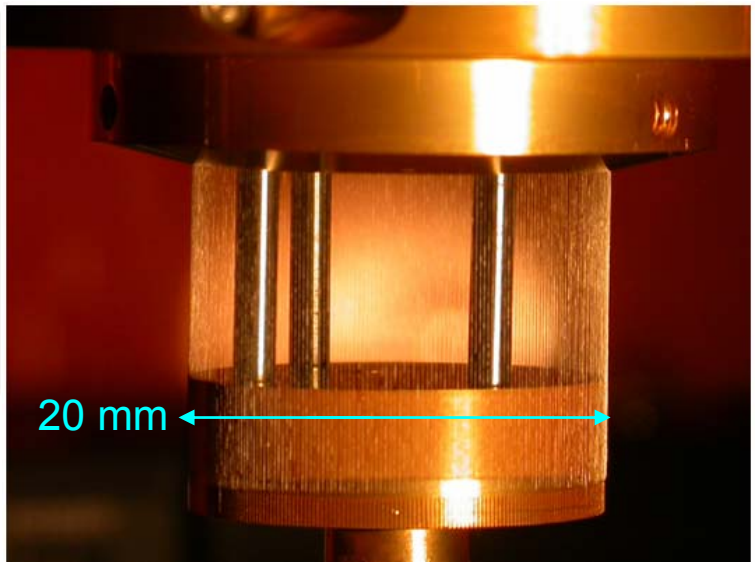

Z Facility: 11.5 MJ Stored, 19 MA
ZR Facility: ~23 MJ Stored, ~26 MA

Peak radiation powers have been obtained using annular wire arrays:

1-1.8 MJ x-ray energy yield

(10-15% conversion efficiency)

100-250 TW x-ray power

General “rule-of-thumb” dichotomy:
Lasers are power-rich, energy-poor
Z-pinches are power-poor, energy-rich

Sandia National Laboratories

High-energy lasers are commonly used as intense line radiation x-ray sources (e.g., for backlighting)

The Z-Beamlet Laser (ZBL) at Sandia was formerly the prototype laser for the 192-beam NIF facility. ZBL is a ~2 TW, multi-kJ laser facility used for x-ray backlighting.

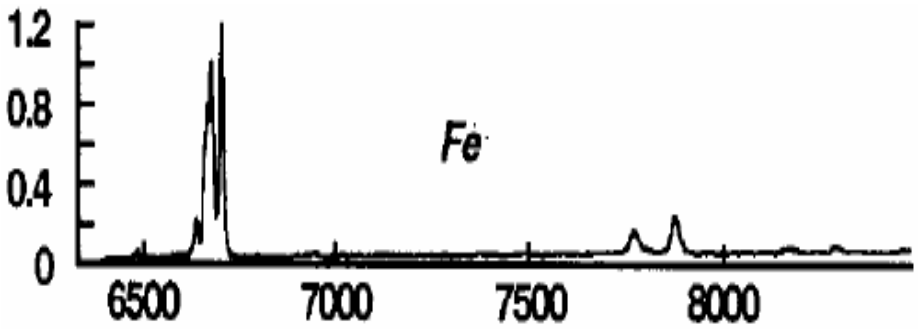

Example x-ray spectrum from an iron target

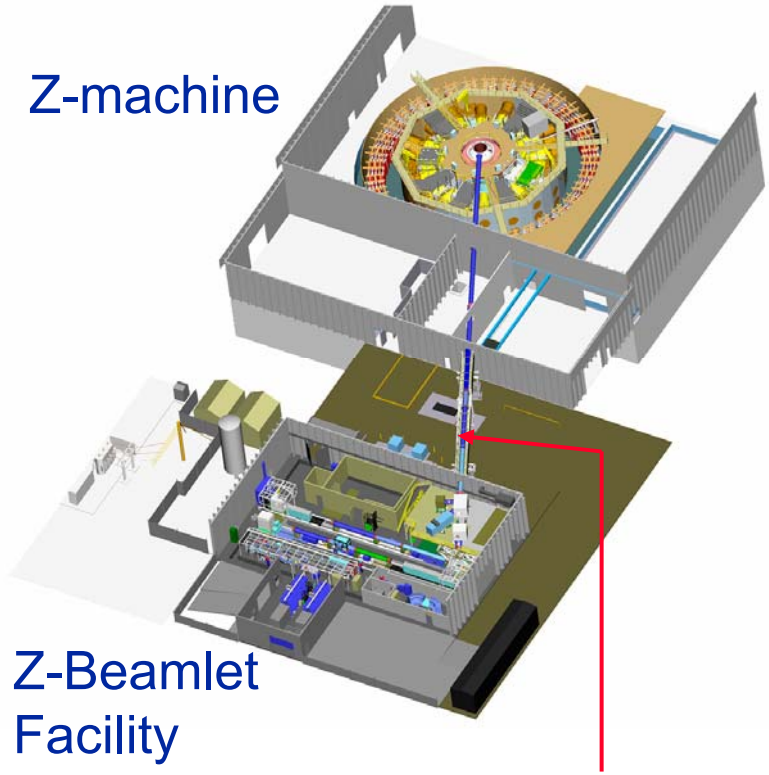

A ~ 75-m-length relay telescope brings the beam to the top of the Z chamber

Sandia National Laboratories

Table of Contents

Using optics with X rays is much more challenging than with optical light

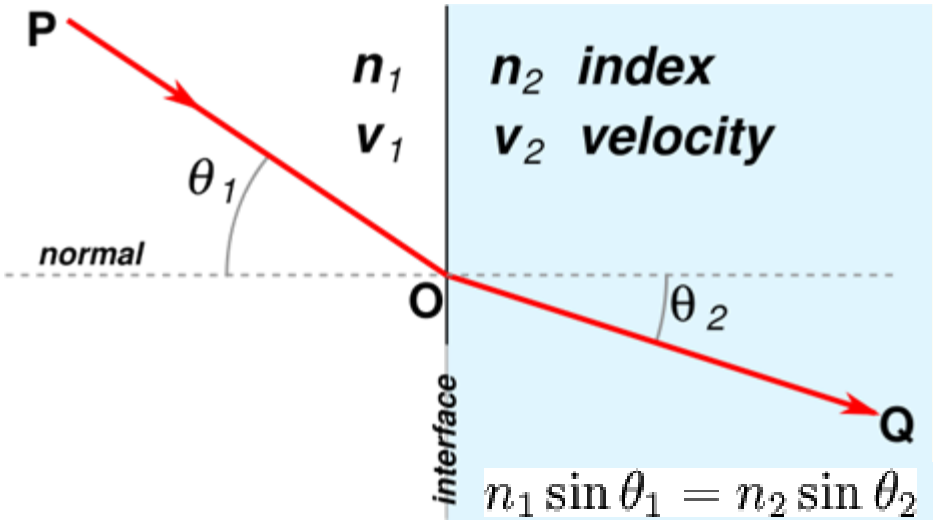

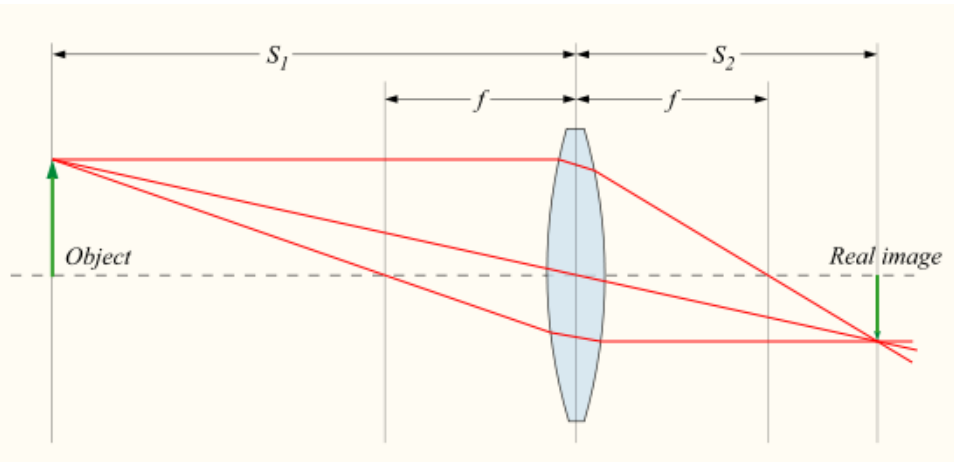

With optical light, one usually takes advantage of refraction in materials to create lenses to focus images

Very complex imaging lens systems can be built to magnify, image, etc.

Index of Refraction for Light (589 nm)
Glass: 1.52-1.66
Water: 1.333
Quartz: 1.544
Diamond (C): 2.417

Index of refraction for X rays

$n=1-\delta-i\beta$

Note real part of n<1!!!

Sandia National Laboratories

Absorption of soft x rays in matter, while useful for radiography, also makes practical lenses difficult

Roentgen's original x-ray image of his wife's hand.

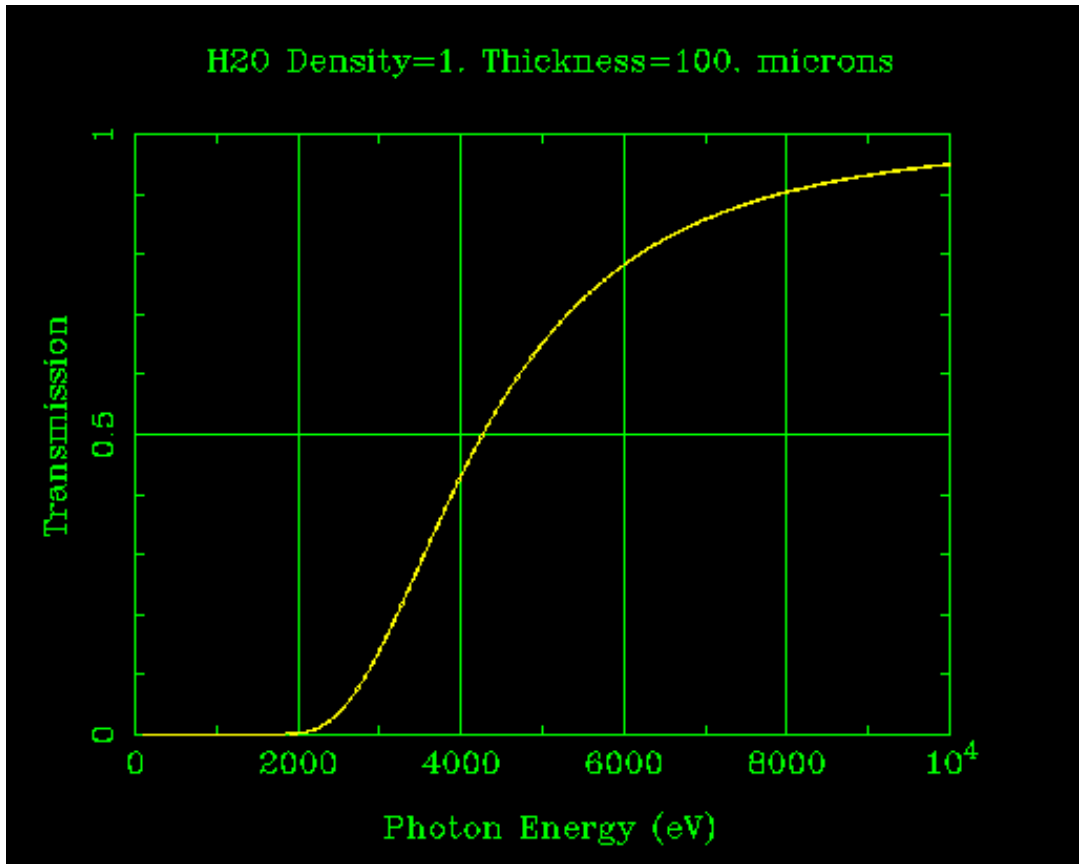

The transmission of x rays through a medium is a function of (1) the material and (2) the x-ray energy

Graph created using: http://henke.lbl.gov/optical_constants/

There are groups building parabolic and capillary lenses for use with 10-100 keV x rays

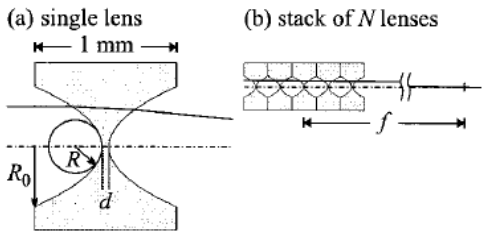

FIG. 1. Schematic sketch of a parabolic compound refractive lens. The individual lenses (a) are stacked behind each other to form a compound refractive lens (b).

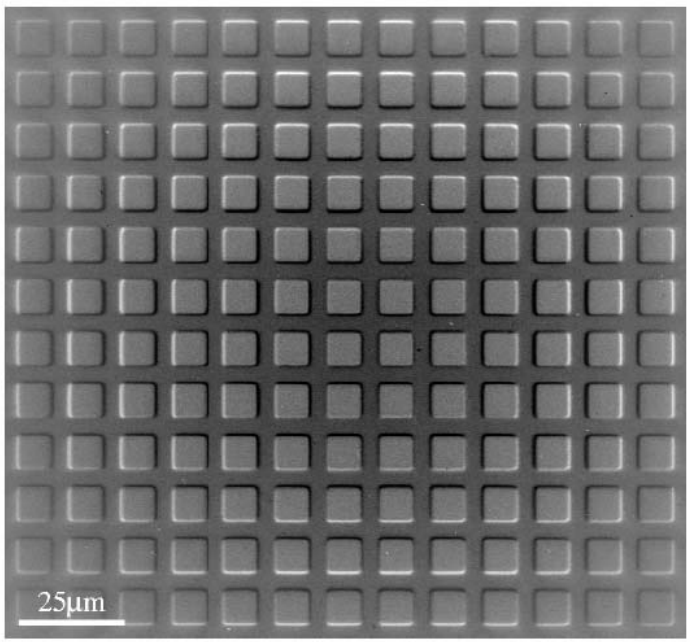

FIG. 1. X-ray micrograph (flat field corrected) of a Ni mesh (2000 mesh) recorded at $E=25$ keV ($N=120$, $f=1048$ mm, $L_1=1098$ mm, and $L_2=23.02$ m).

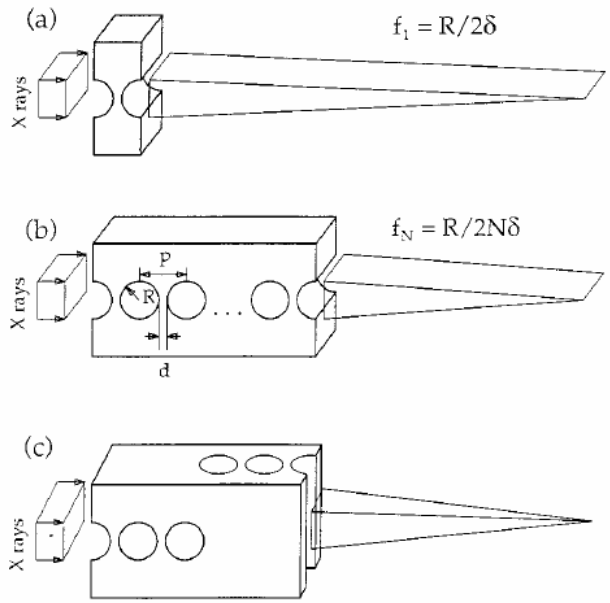

Fig. 1. Schematic view of the compound refractive lens as an array of air (vacuum) cylindrical holes: R, radius of the holes; d, minimum spacing between the holes; N, number of holes; λ, wavelength of x rays to be focused; f, focus distance; δ, decrement of the refractive index of the lens material; p, distance between the centers of the two neighboring holes: (a) single refractive lens, (b) compound refractive lens for linear focusing, (c) compound refractive lens for two-dimensional focusing in crossed geometry.

Example references:

B. Lengeler *et al.*, Appl. Phys. Lett. 74, 3924 (1999).
A. Snigirev *et al.*, Appl. Optics 37, 653 (1998).
C.G. Schroer *et al.*, Rev. Sci. Instrum. 73, 1640 (2002).

It is also possible to create lenses based on x-ray diffraction (Fresnel Zone Plates)

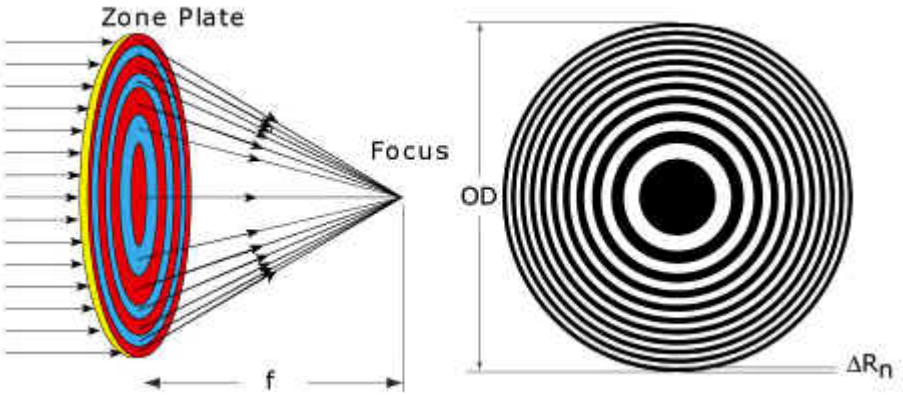

Zone plates use constructive interference of light rays from adjacent zones to form a focus. The focal length f of a zone plate is a function of its diameter OD, its outermost zone width ΔRn and the x-ray wavelength λ.

$$f = OD\Delta Rn / \lambda$$

The field of view of the zone plate is determined by its diameter.

The resolution of a zone plate is limited to 1.22 ΔRn (Rayleigh criterion) requiring narrow zones for best performance.

It is difficult to make high-resolution zone plates of a sufficient size (diameter) that allow large fields of view.

Example commercial source for zone plates: http://xradia.com/index.html

Grazing-incidence Reflection

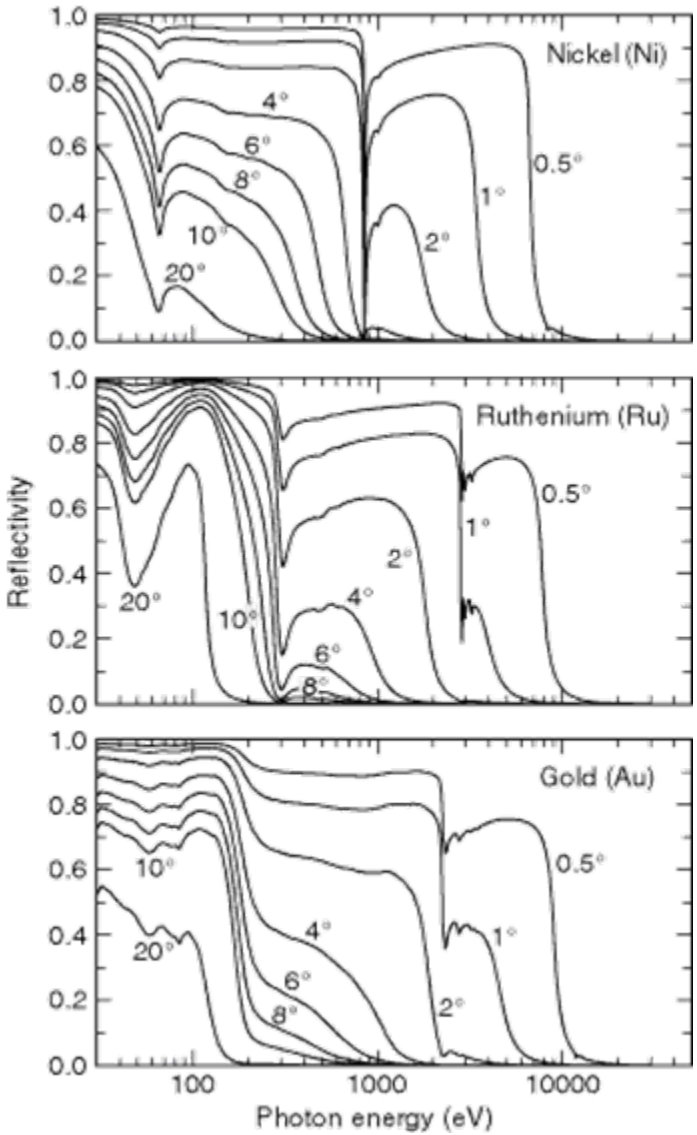

For small angles of incidence off of smooth, thick surfaces it is possible to obtain a high reflectivity at low photon energies. Thus, grazing-incidence optics can be used as mirrors in low-energy optical systems. (e.g., Kirkpatrick-Baez lens)

Because of the high-energy roll off, grazing-incidence mirrors can also be used to eliminate the contribution of high-energy photons to images.

B. L. Henke, E. M. Gullikson, and J. C. Davis, "X-Ray Interactions: Photoabsorption, Scattering, Transmission, and Reflection at E = 50–30,000 eV, Z = 1–92," *At. Data Nucl. Data Tables* **54,** 181 (1993).

Mirror reflectivites can be calculated at: http://henke.lbl.gov/optical_constants/

Planar crystalline structures can be used as x-ray mirrors

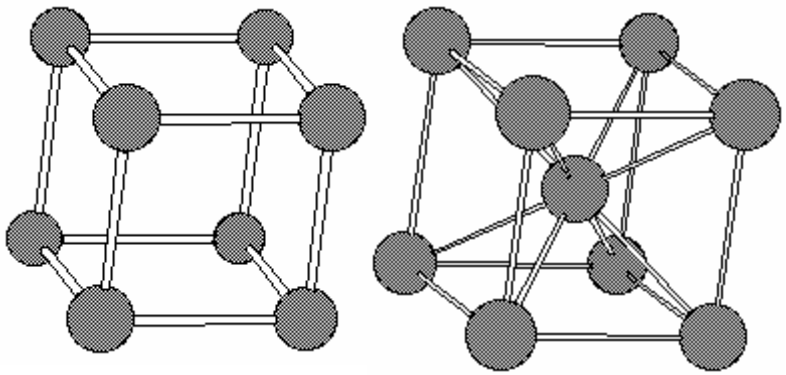

Crystals have a wide variety of periodic structures. Many planes of atoms can be formed that cut through the basic lattice along different orientations

These orientations can be labeled using a notation known as “Miller indices,” which specify how the planes cut through the basic crystal lattice.

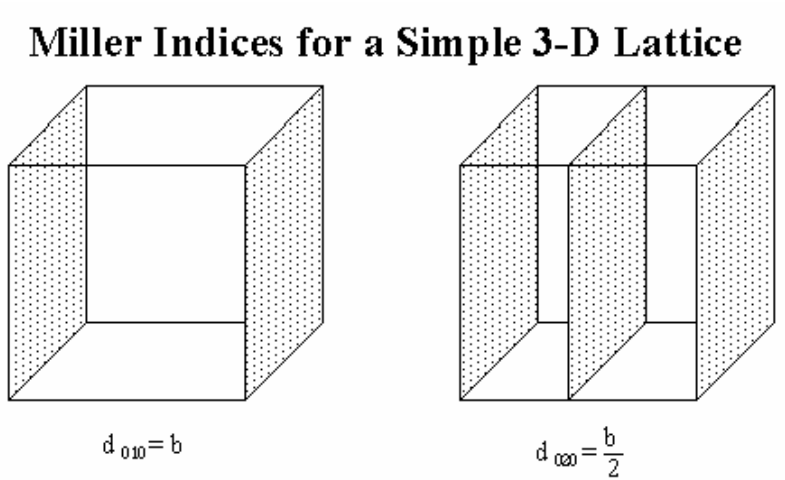

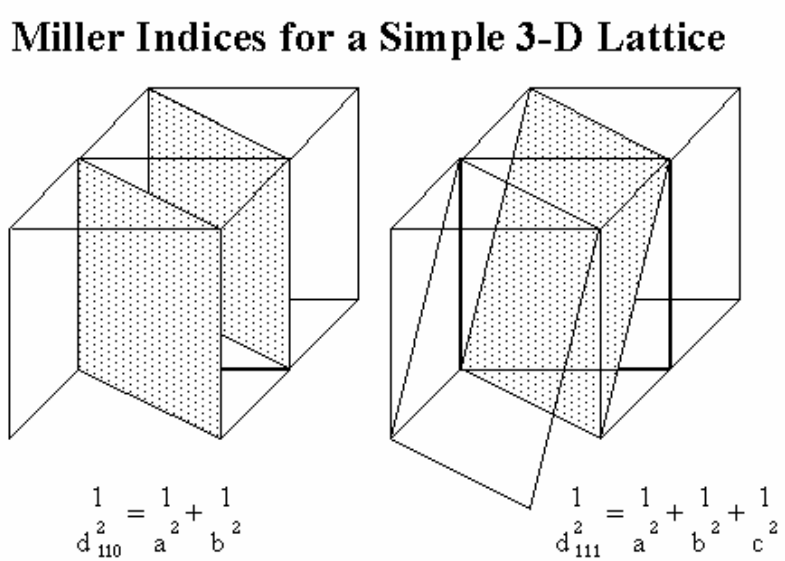

Lattice figures from http://wb.chem.lsu.edu/htdocs/people/sfwatkins/MERLOT/lattice/

Only x rays satisfying the Bragg Equation reflect from planes in the crystal

- **If photons of a specific wavelength reflect from a large number of crystal planes, only photons with the following wavelengths will be reflected:**

  $n\lambda = 2d \sin(\theta)$

  n = Integer reflection order
  λ = Photon wavelength
  d = Crystal plane spacing
  θ = Bragg angle

- **2d spacings of crystals are in the 1.624-26.6 Å range* (7.6-0.466 keV E_{min})**

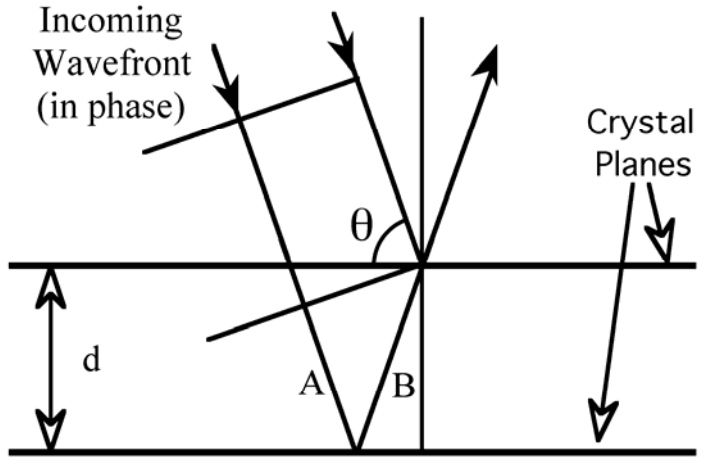

$A = d / \sin(\theta) - 2d \cos(\theta) / \tan(\theta)$

$B = d / \sin(\theta)$

Total path length difference = $A + B = 2d \sin(\theta)$

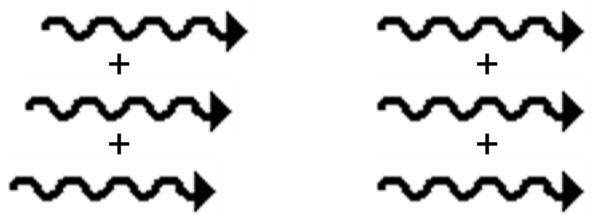

Destructive Interference

Constructive Interference

* X-ray Data Booklet (http://xdb.lbl.gov/)

Sandia National Laboratories

Flat crystals can be used as x-ray mirrors or as x-ray spectrographs, depending on the dimensions

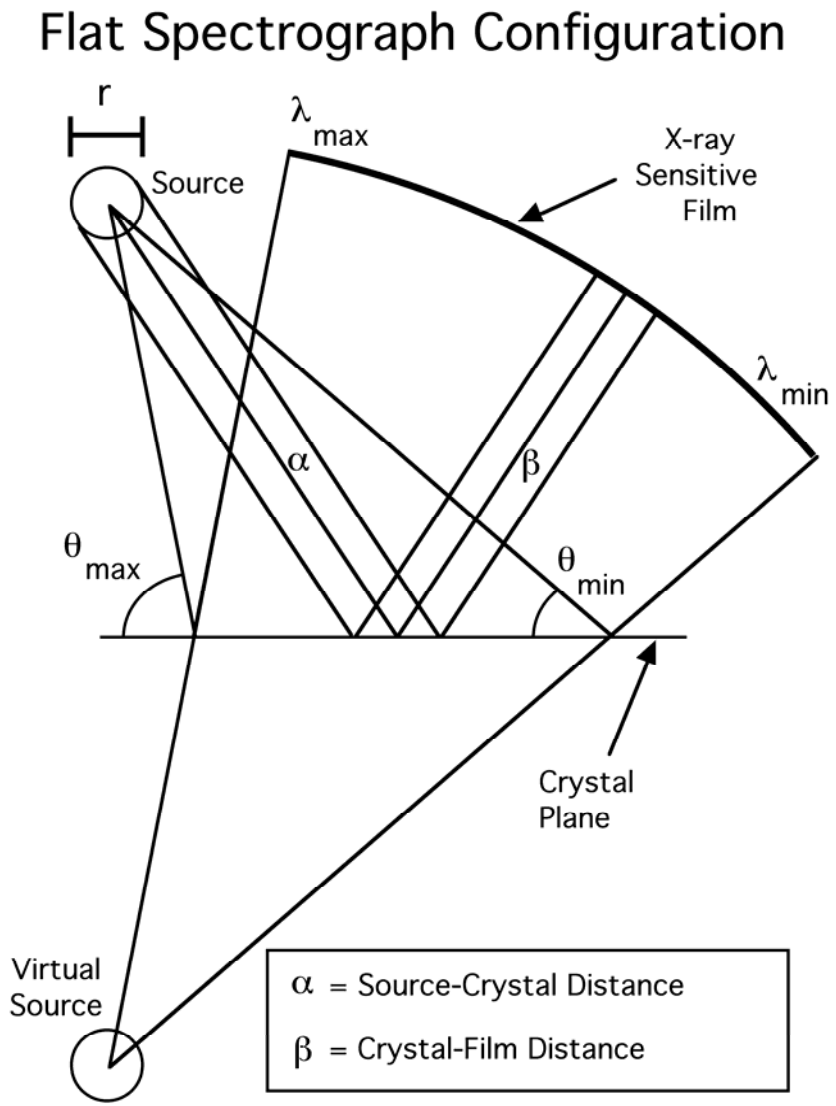

- If the angle of incidence of the x rays varies considerably, then the mirror is effectively a spectrograph
- To use crystals as true x-ray mirrors in imaging, the Bragg angle ideally changes little over the image
- By bending the crystals, one can change the range of Bragg angles and create monochromatic images
- With an array of pinhole images (see later slides) it is possible to create monochromatic images at multiple wavelengths simultaneously

Table of Contents

Pinhole Camera Imaging

X-ray Pinhole Camera

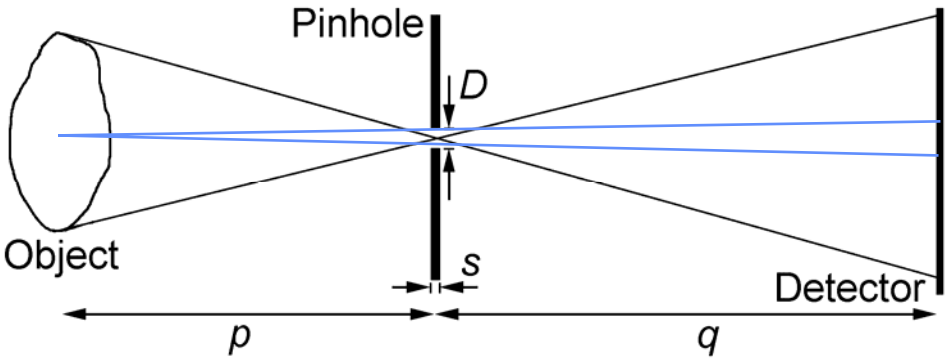

$$\sigma^2 \approx \sigma_{geom}^2 + \sigma_{diff}^2 = \left(\frac{(M+1)D}{M}\right)^2 + \left(\frac{2.44\lambda p}{D}\right)^2$$

Pinhole imaging is a simple way to take x-ray photographs that does not involve the use of optics (e.g., lenses, mirrors)

The geometric resolution of a pinhole system depends on the magnification and the pinhole diameter, and the field of view is limited by the relative dimensions of the detector and imaging system.

For small enough pinholes, x-ray diffraction becomes the limiting factor in the resolution, especially for low-energy photons.

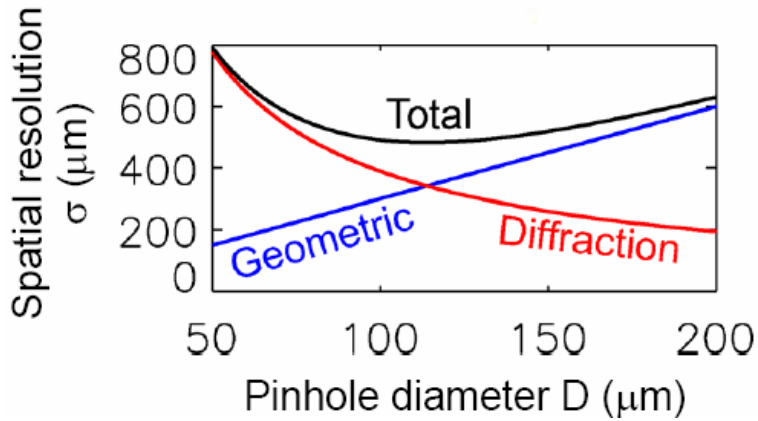

Example 277 eV pinhole imaging system calculations (B. Jones, Sandia)

Sandia National Laboratories

Time-gated pinhole images are obtained using micro-channel plate detectors (MCPs)

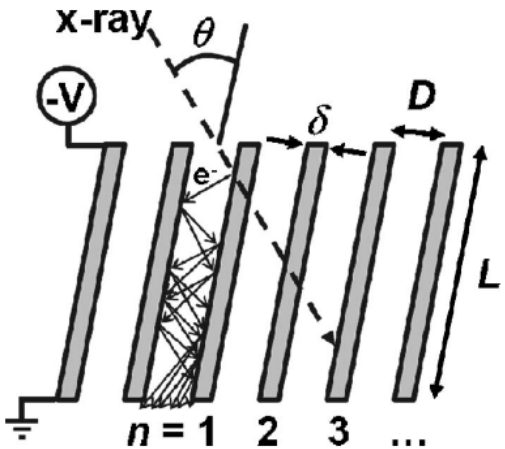

FIG. 1. Cross-sectional schematic illustration of the MCP operation for x-ray detection.

MCPs amplify the signal from individual x-ray photons, making them high-sensitivity. By time-gating the bias pulse one can create a time-gated detector.

- Time resolutions ~0.1-10 ns can be achieved using MCPs.
- The spatial resolution of the output is limited by the tube diameter and x-ray penetration, and is usually ~100 μm.
- When used over broad spectral ranges the intrinsic response of the MCP can make quantitative analysis difficult.

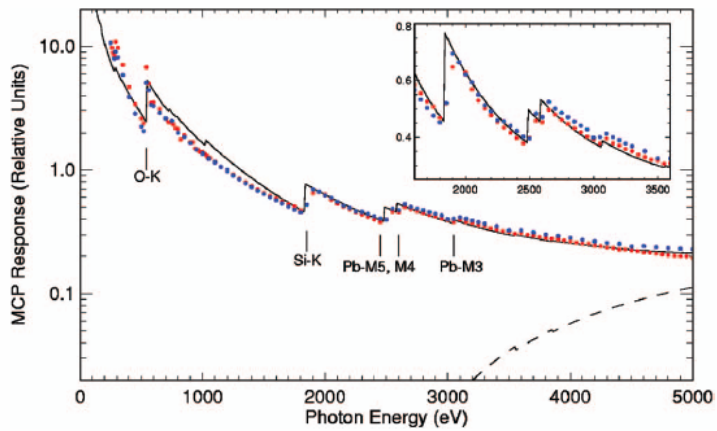

FIG. 3. (Color) Relative MCP response as measured for two separate detector systems (red and blue dots) and as calculated from the model in Eq. (5) (solid line) using the material fractions determined from XPS analysis of the MCP composition. The dashed line gives the calculated contribution to the MCP response from electrons produced everywhere, except the front surface of the first channel wall.

Example Reference articles:
*Rochau *et al.*, Rev. Sci. Instrum. 77, 10E323 (2006).
Katayama *et al.*, RSI 62, 124 (1991).
Bradley *et al.*, RSI 63, 4813 (1992).
Ze *et al.*, RSI 63, 5124 (1992).
Nash *et al.*, RSI 70, 464 (1999).
Oertel *et al.*, RSI 72, 701 (2001).

Spectral resolution of x-ray pinhole cameras is usually limited using simple filters

- **A Ross filter is a pair of filters with similar transmissions over most of the spectral range**
- **In principle, the two signals can be subtracted and the difference is due solely to contributions from the range where the filters have different transmissions.**

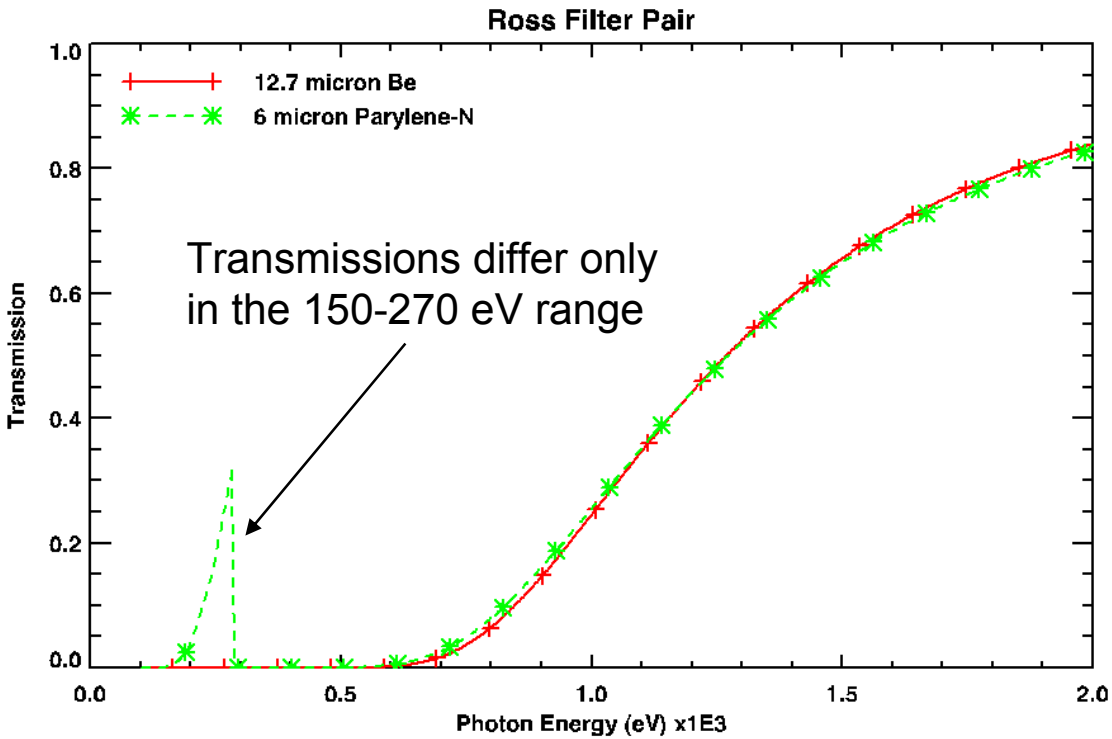

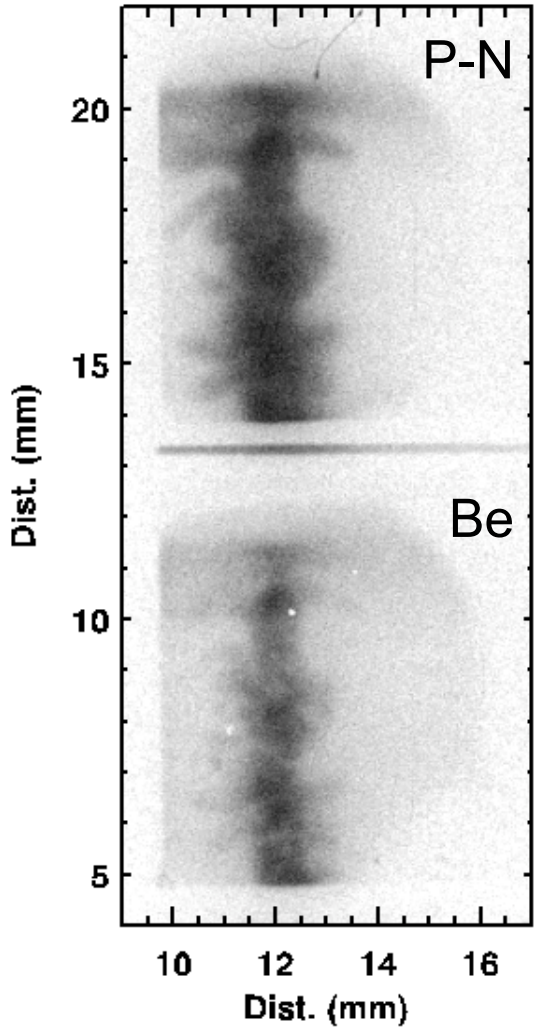

Sandia National Laboratories

Example Pinhole Camera Data from Z

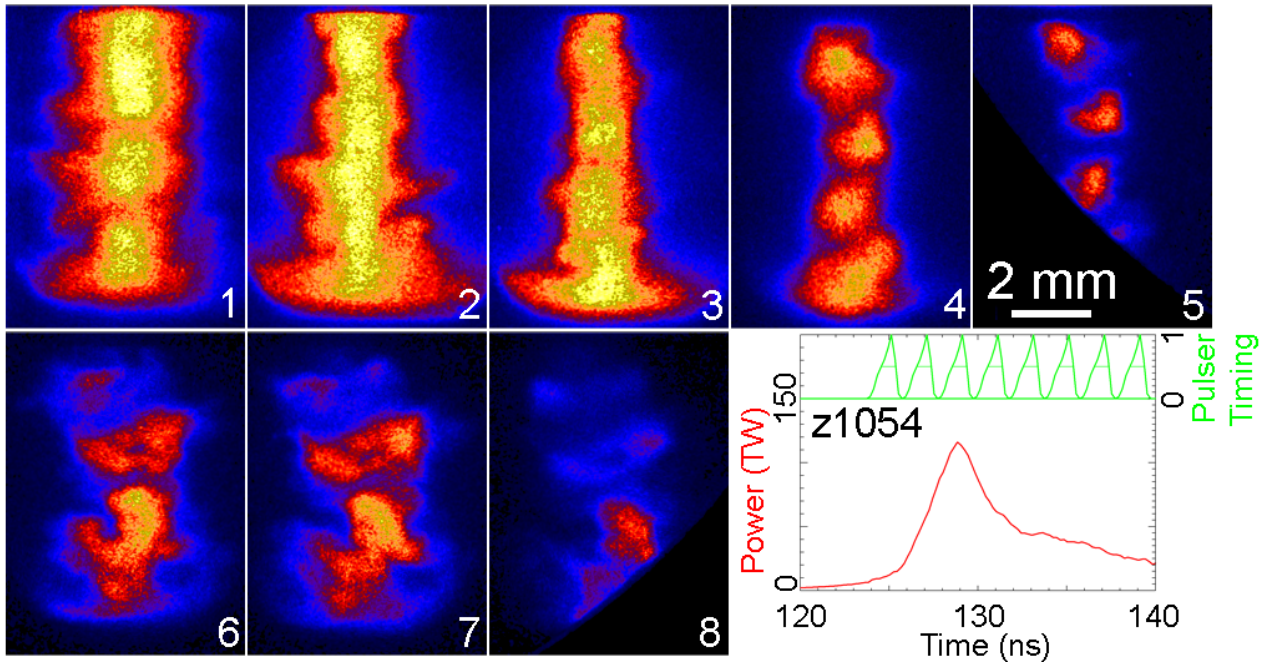

Used an 8-frame, 1-ns gated microchannel plate detector system to capture the self-emission from a tungsten wire-array z-pinch implosion through a 12.7 μm Be filter (>1 keV).

Frames straddle the peak of the x-ray emission and show the pinch going unstable after the peak emission.

A pinhole camera can be combined with a grazing-incidence mirror to limit the spectral range*

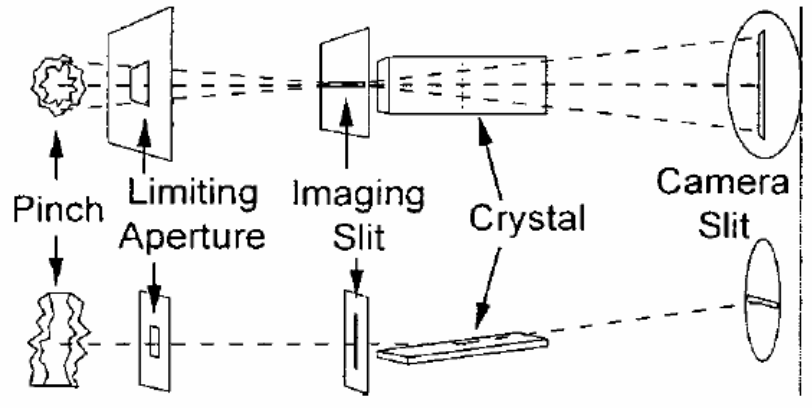

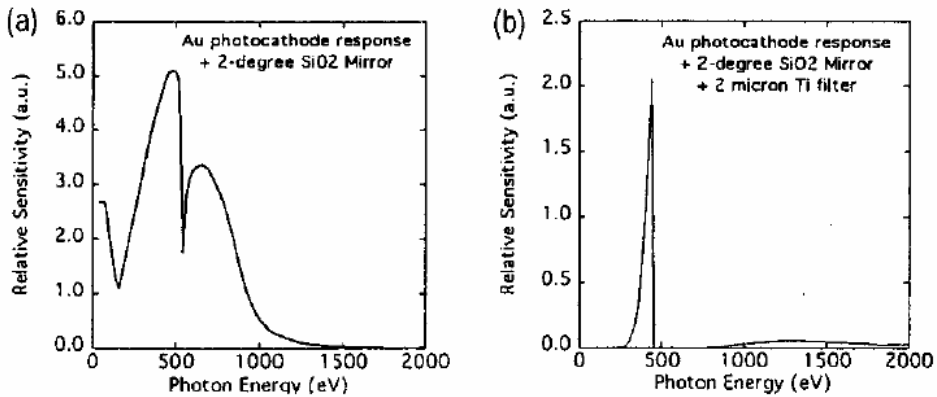

FIG. 3. (a) The relative response of the x-ray streak camera taking into account the Au photocathode response and the 2° SiO_2 mirror. (b) The relative response shown in (a), adjusted for the addition of a 2 μm Ti filter to the system. This combination successfully eliminates contributions from >1 keV x-rays.

For a fixed angle, the mirror has a high-energy cutoff that can eliminate the contribution from high energy photons.

With a judicious choice of filter material (one that has an edge at a relevant spectral location), one can create an instrument with a very narrow spectral band.

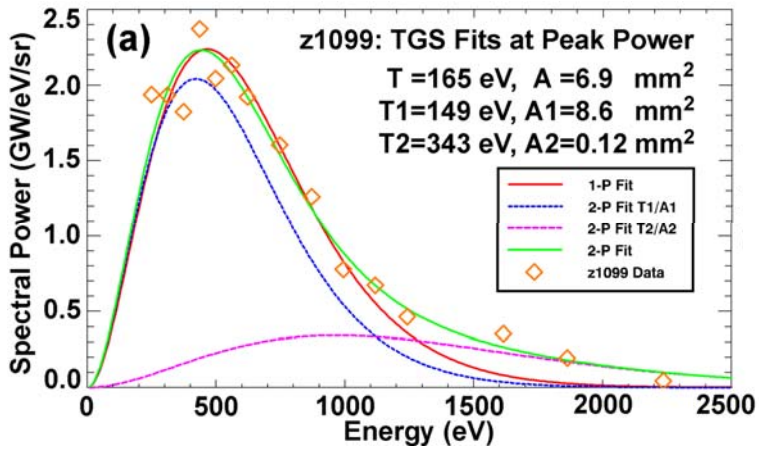

*e.g., D.F. Wenger *et al.*, Rev. Sci. Instrum. 75, 3983 (2004).

Sandia National Laboratories

Example z-pinch self-emission data* from a grazing-incidence streak camera system

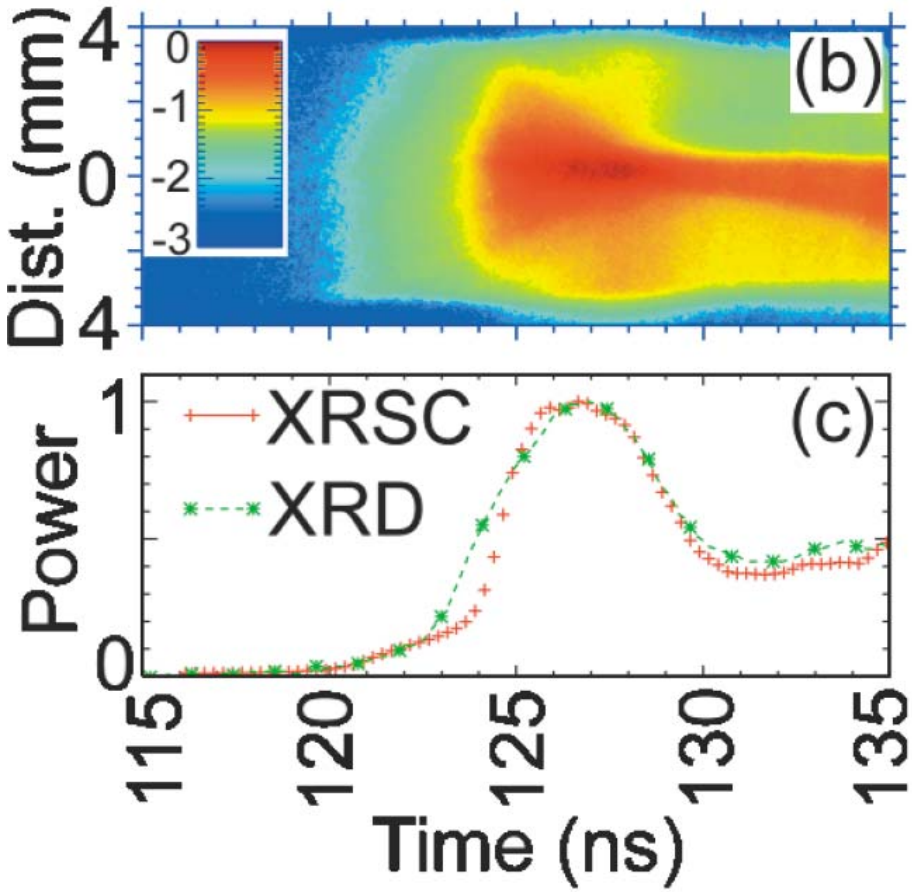

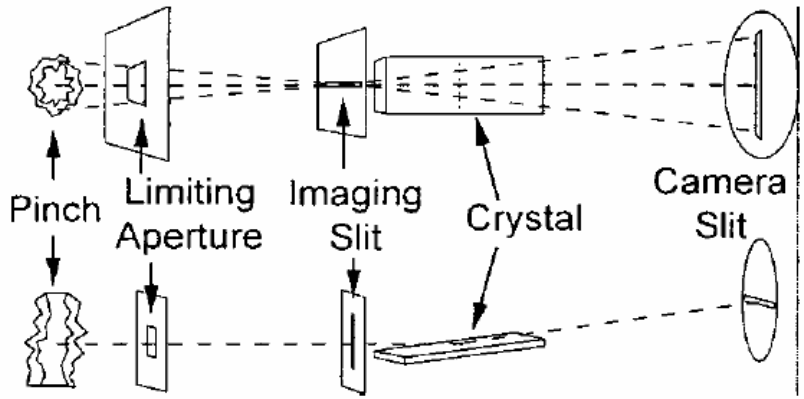

The spectral response of the instrument was tuned to match the peak of the blackbody emission spectrum.

X-ray emission from the pinch was tracked as a function of time and 1-D space.

*D.B. Sinars *et al.*, Phys. Rev. Lett. 93, 145002 (2004).

Multi-layer mirrors (MLMs) act as "artificial crystals" and can be used to provide monochromatic images

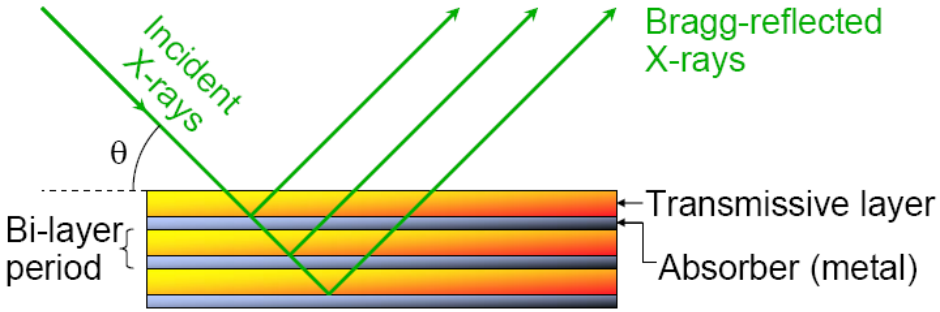

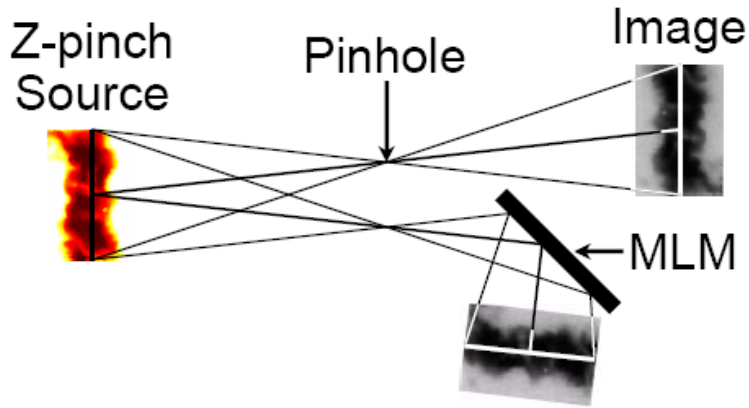

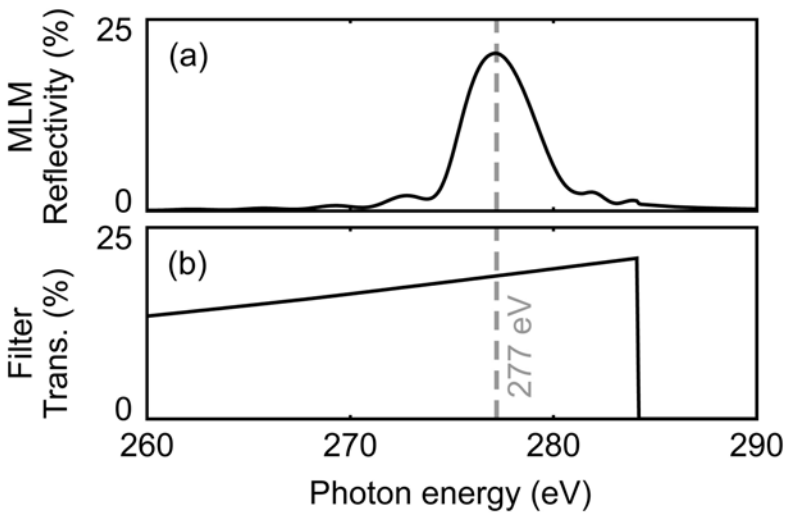

- A 277 eV camera* was made for the Z-machine using a planar Cr/C multilayer mirror.
  - ~5 eV bandwidth, 20% peak reflectivity
  - 34º grazing angle
- 4 μm Parylene-N + 1000 Å Al filter blocks second-order (higher-energy) reflections

B. Jones *et al.*, IEEE T. Plasma Sci. 34, 213 (2006).

Sandia National Laboratories

Example multilayer mirror pinhole camera on Z/ZR

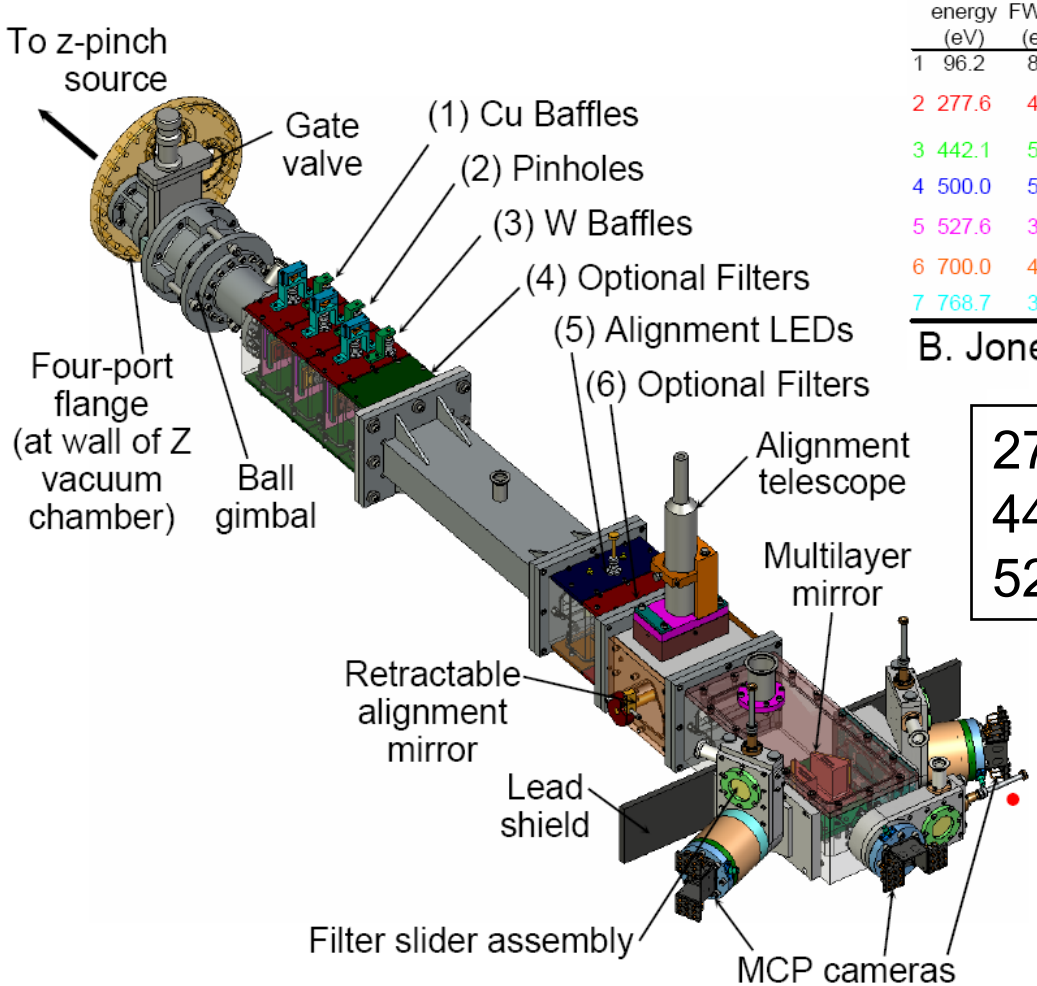

B. Jones *et al.*, Rev. Sci. Instrum. **75**, 4029 (2004).

	Photon energy (eV)	FWHM (eV)	Peak R (%)	Multilayer materials	Bi-layer period (Å)	N	Γ	σ (Å)	Filter	Spatial resolution (μm)	Optimal pinhole diameter (μm)
1	96.2	8.3	59.9	Mo/Si	125	75	0.4	4	2.5 μm Be	835	197
2	277.6	4.2	24.1	Cr/C	40.42	75	0.335	3.70	4 μm Parylene-N + 1000 Å Al	482	114
3	442.1	5.4	4.1	W/Si	25.35	120	0.243	3.28	1 μm Ti	382	90
4	500.0	5.0	4.9	W/Si	22.375	120	0.24	3	1 μm V	359	85
5	527.6	3.9	5.1	W/Si	21.18	175	0.196	2.86	1 μm Cr	350	82
6	700.0	4.3	4.2	W/Si	15.935	175	0.3	3	1 μm Fe	304	72
7	768.7	3.0	4.4	W/Si	14.5	450	0.31	3	1 μm Ni	290	68

B. Jones *et al.*, Rev. Sci. Instrum. **77**, 10E316 (2006).

277 eV camera built on Z
442 eV camera to be added on ZR
528 eV camera built on SATURN

Sandia National Laboratories

Example multilayer mirror pinhole camera data of Cu wire-array implosion on Z

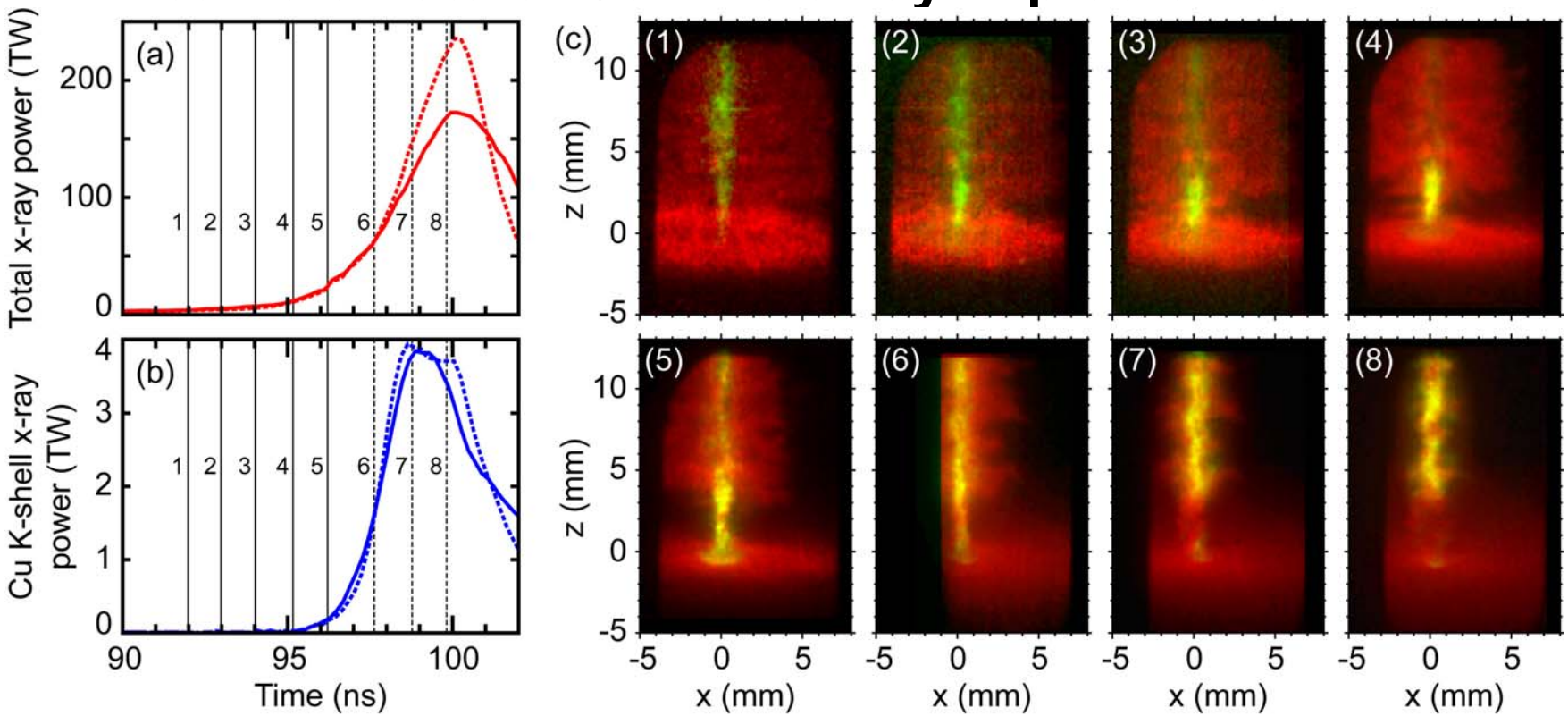

(a) Total radiated x-ray power and (b) ~8 keV Cu K-shell x-ray power with associated imager frame timing indicated for Z shots 1616 (dashed lines) and 1617 (solid lines). (c) False-color overlay of 277 eV (red) and Cu K-shell (green) self-emission images. Yellow indicates both 277 eV and K-shell emission superimposed. MLM-reflected images track the implosion of cooler trailing mass, which accretes on axis where K-shell emission is excited.

(Figure courtesy of B. Jones, Sandia)

Bent crystals can be used as high-resolution, monochromatic self-emission microscopes

- **Using crystal mirrors bent to spherical or toroidal shapes, can achieve point-to-point focusing between object and detector**
- **Spatial resolution is essentially limited by the crystal quality and high-order astigmatism. Spatial resolutions ~10 μm possible.**
- **If spherical crystals are used, then useful Bragg angles 80º<θ<90º (with toroidal crystals 70º<θ<90º)*. This constrains λ to values near 2d spacings of natural crystals [sin(80º)=0.985, sin(70º)=0.94]**

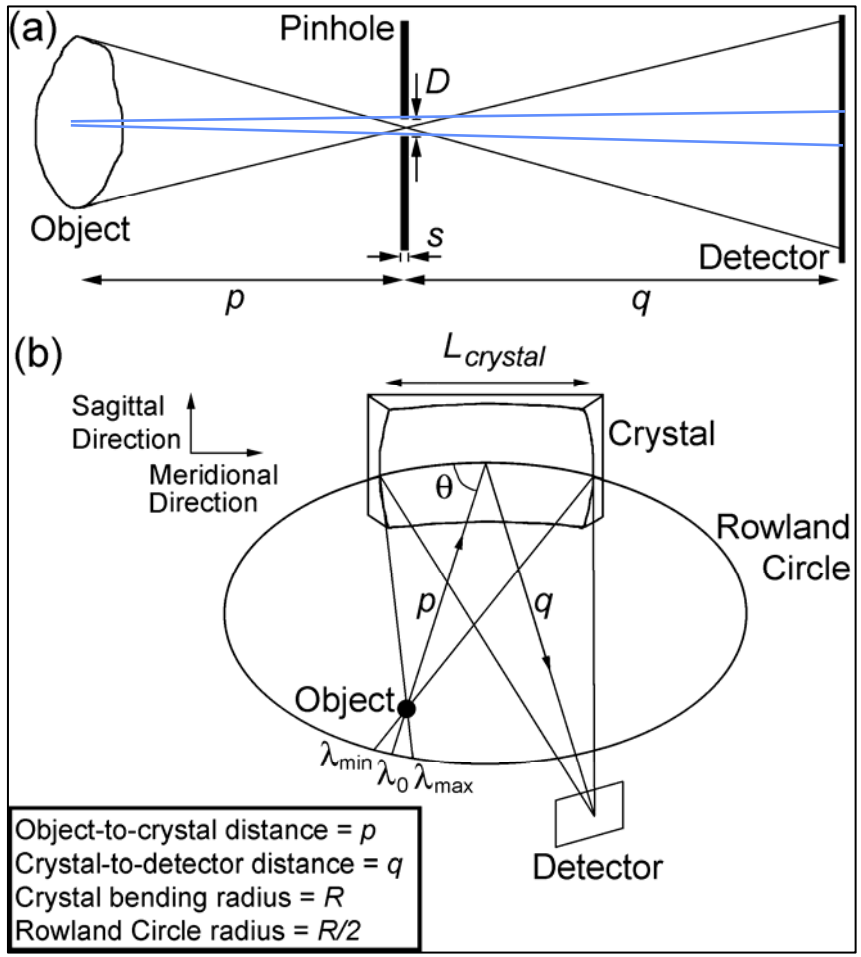

Self-emission Imaging Geometries

* J.A. Koch *et al.*, Appl. Optics 37, 1784 (1998).

Sandia National Laboratories

Example 6.15 keV self-emission images from tungsten wire-array implosions on Z

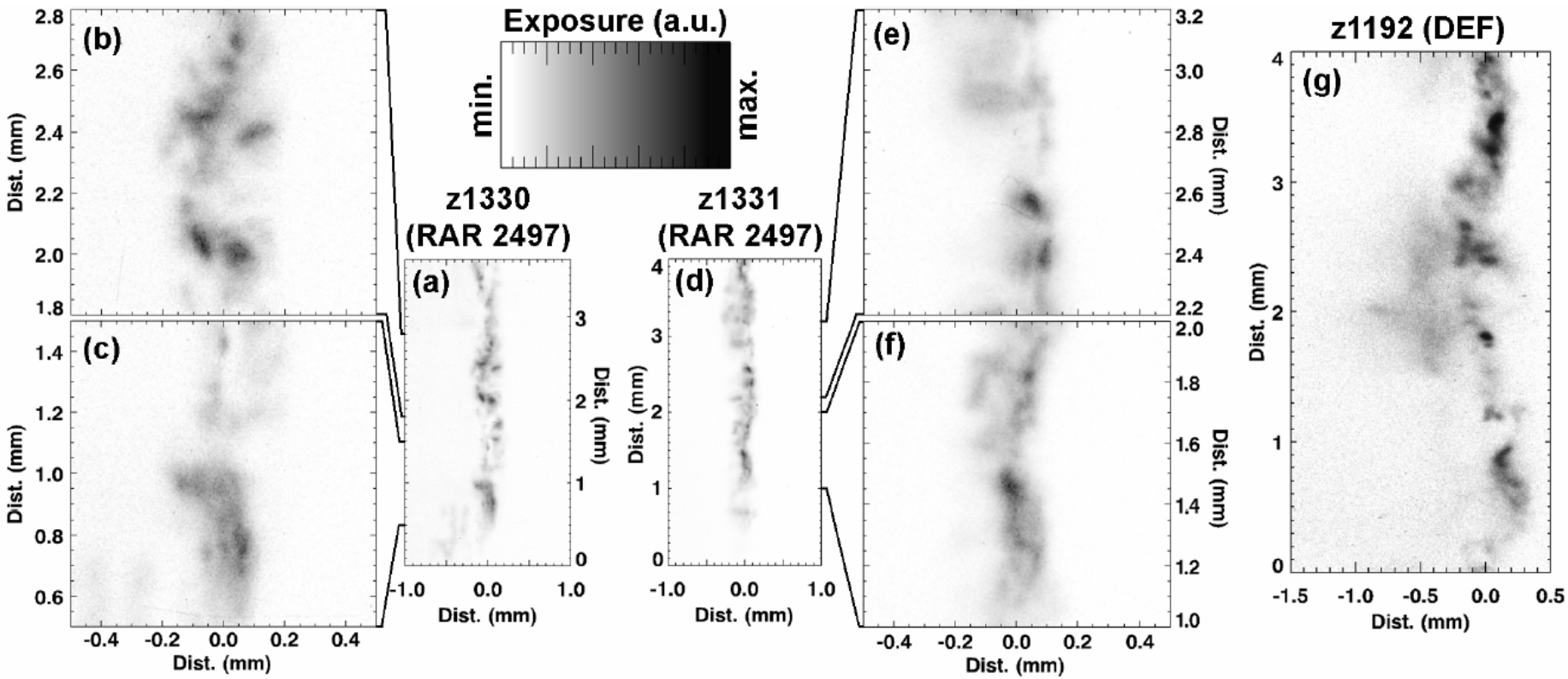

FIG. 2: Time-integrated 6151 eV self-emission images from three example tests. On these tests either the backlighter exposure on the first film was too low to be seen (parts (a)-(f)) or there was no backlighter source (part (g)). The film exposure levels of each image were adjusted to provide useful contrast for these figures. A wall in the return-current canister blocked any self-emission from regions $\geq$0.4 mm.

Table of Contents

Sandia National Laboratories

Point-projection backlighting using Z-Beamlet

- **Simplest, most energetically efficient method for backlighting**
  - **Small source enhances conversion efficiency into x rays (vs. areal backlighting)**
  - **No complex optics or alignment required**
- **Disadvantage for HEDP applications**
  - **X rays and debris from object have direct line of sight to detector**
  - **Resolution depends on x-ray source size—can't focus ~1 kJ of laser energy into a arbitrarily small spot**
- **X spectrum used for backlighting depends on laser target material**
  - **Typically K-shell (He-like) sources are used**
  - **Examples: Ti (4.7 keV), Fe (6.7 keV), Zn (9 keV)**
- **Conversion efficiency decreases with increasing photon energy***

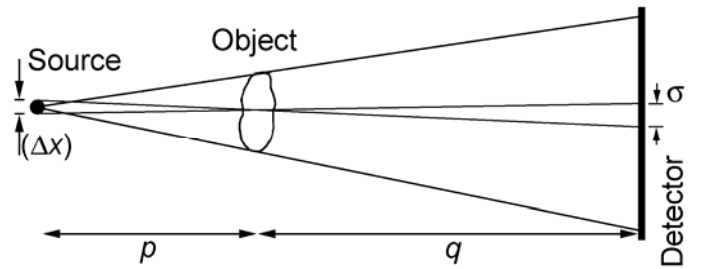

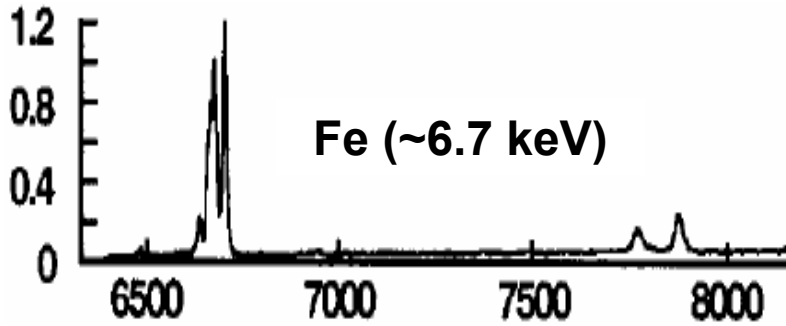

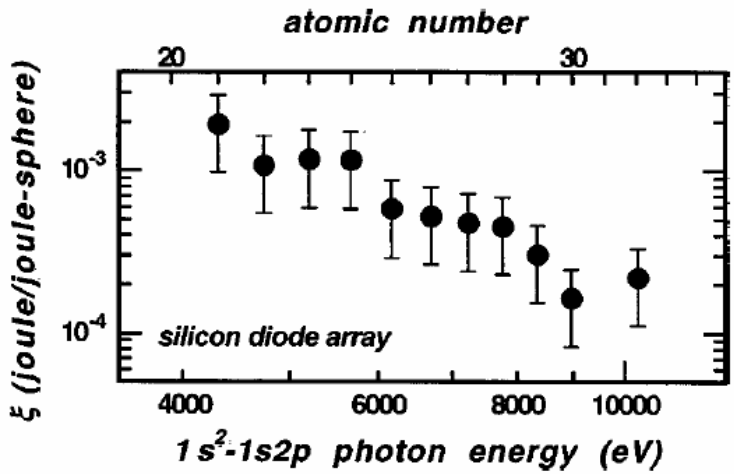

* L.E. Ruggles *et al.*, Rev. Sci. Instrum. 74, 2208 (2003).

Radiography on Z uses the Z-Beamlet Laser*

- Z-Beamlet resides in a separate facility to the south of Z. The beam travels 75 m via a relay telescope to a final optics assembly on Z
- Two different Final Optics Assemblies (FOAs) are available:
  - Off-axis FOA: Fixed focal spot position 1 m from the Z-machine axis, used for point-projection imaging
  - On-axis FOA: Variable focal spot position (0.1-0.2 m from axis), used for curved-crystal imaging
- In a single 0.3-1.5 ns pulse, the laser can deliver up to 1.5 kJ of 527-nm light to a target in a 50-200 μm spot (>10^{15} W/cm^2 on target) to produce ~0.1-10 J of x rays for backlighting
- Up to 4 such pulses can be generated within a 20 ns time window

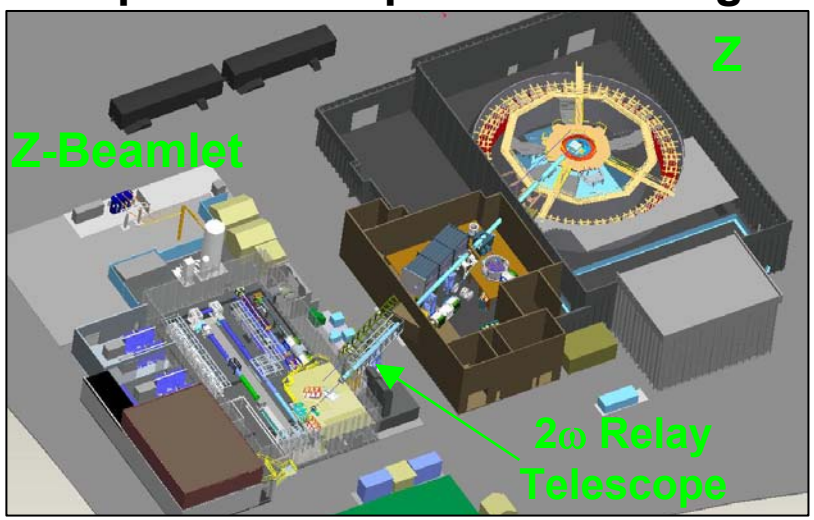

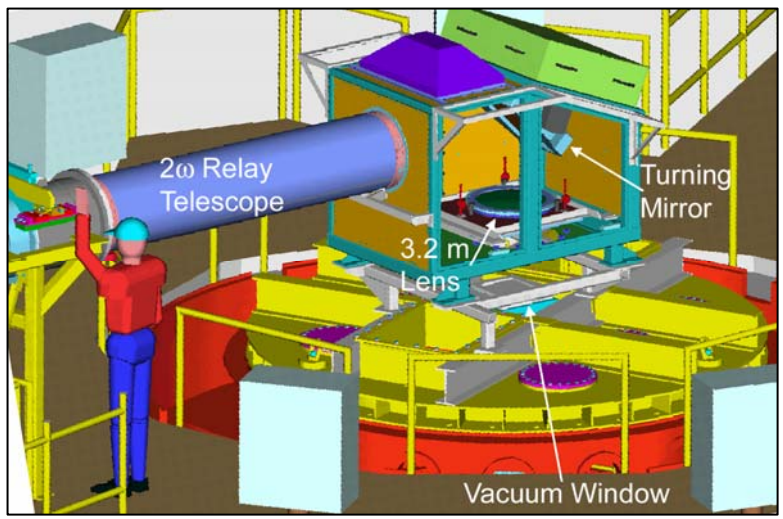

* P. Rambo *et al.*, Appl. Optics 44, 2421 (2005).

Example data: point-projection backlighting was used to study ICF capsule implosions*

Initial 6.7 keV imaging used a 4.8x imaging geometry with a large laser focal spot size

Improved 6.7 keV system used 1.7x imaging with 100 μm spot sizes to yield 50 μm spatial resolution

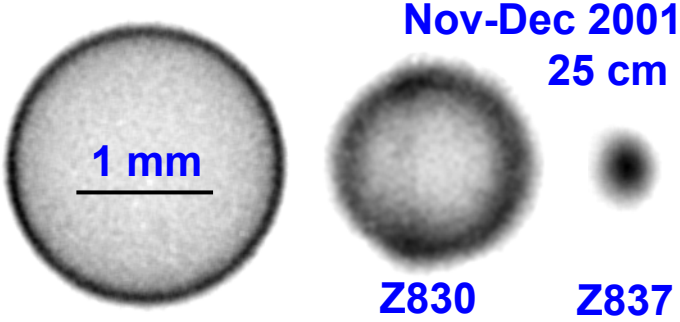

Nov-Dec 2001 [4.8x, 3.2 m lens, 25 cm x 25 cm aperture]

May-June 2002 [1.69x, 2 m lens, 34 cm x 34 cm aperture]

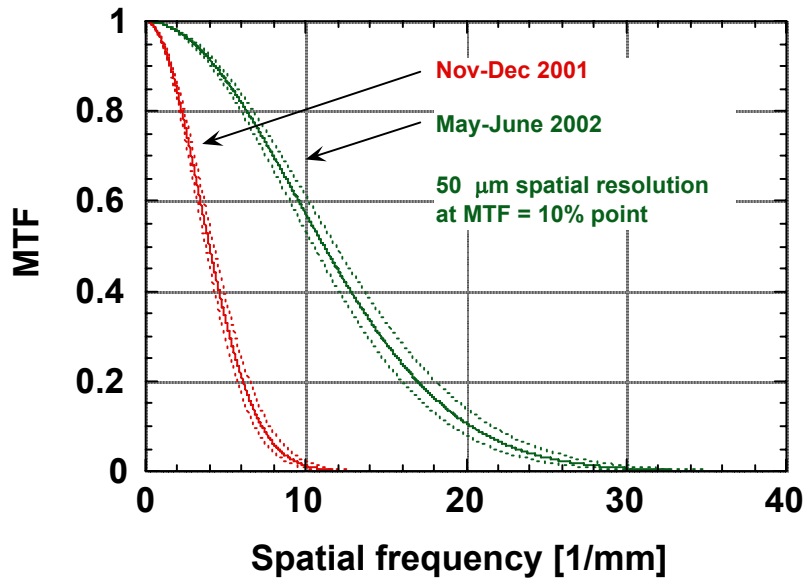

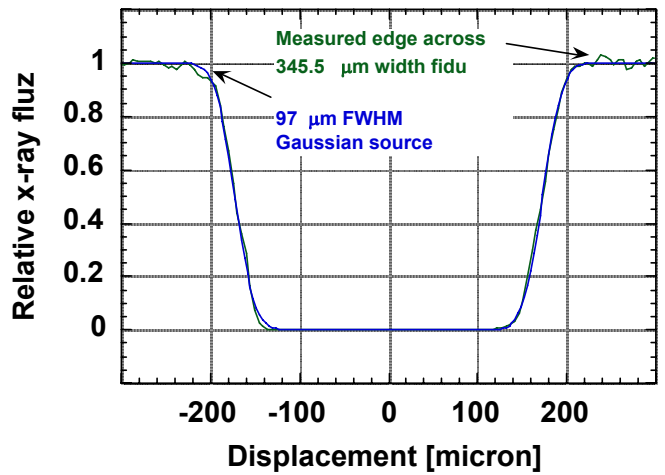

* G.R. Bennett *et al.*, Phys. Rev. Lett. 89, 245002 (2002).

Bent crystals can be used for high-resolution, monochromatic radiography and noise rejection

- As with crystal microscopy, can obtain near point-to-point focusing between object and detector
- In most cases, the image resolution is independent of the source size
- Unlike point-projection, high magnifications are possible
- A limiting aperture can be placed at the focal point of the source to eliminate direct line of sight of debris and background from object to the detector.

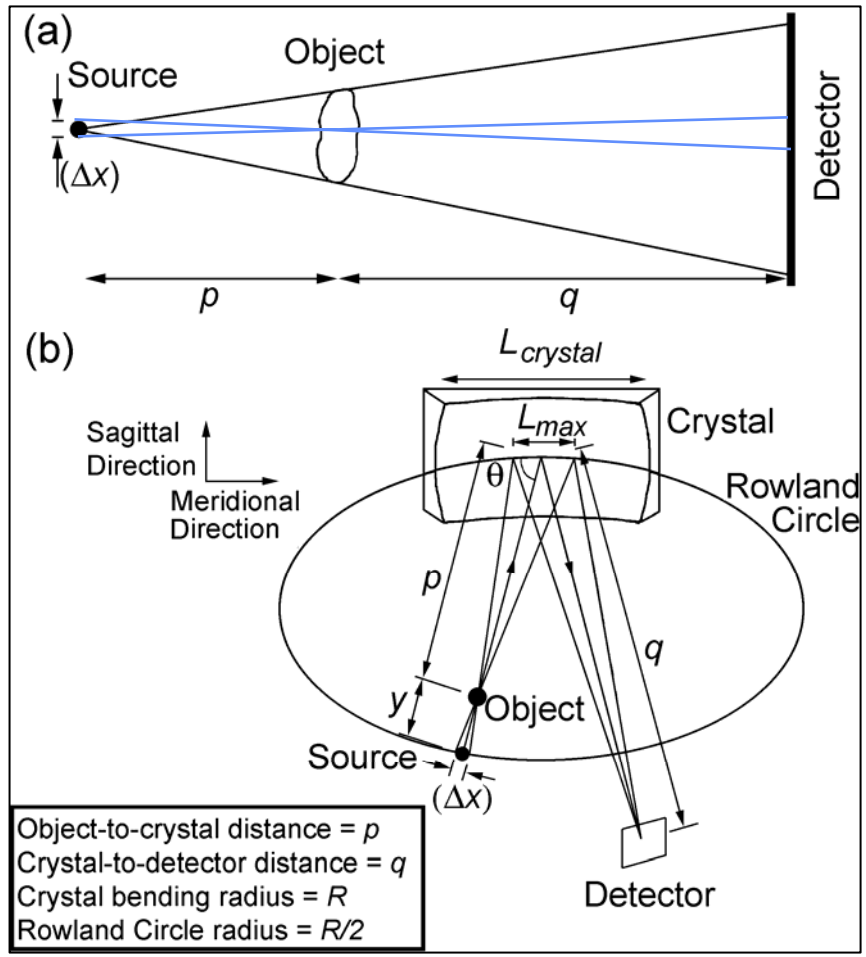

Backlighting Geometries

Curved-crystal imaging offers an elegant solution for backlighting in hostile environments

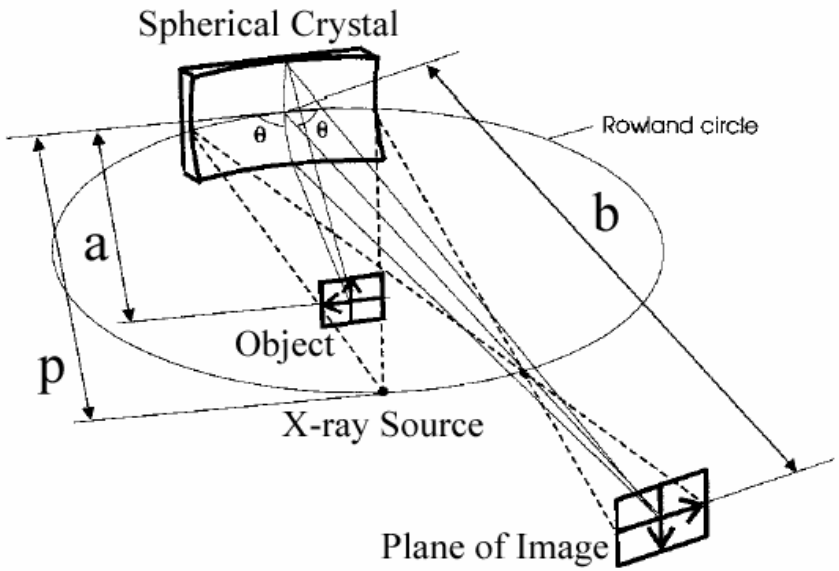

Bent-crystal Imaging

- **Monochromatic (~0.5 eV bandpass)**
- **10 micron resolution**
- **Large field of view (e.g. 20 mm x 4 mm)**
- **Debris mitigation**

- **Concept proposed in mid-1990s.**
  - S.A. Pikuz *et al.*, Rev. Sci. Instrum. **68**, 740 (1997).
- **A 1.865 keV backlighter built at NRL**
  - Y. Aglitskiy *et al.*, Rev. Sci. Instrum. **70**, 530 (1999).
- **Crystal imaging techniques proposed for microscopy/backlighting on NIF**
  - J.A. Koch *et al.*, Rev. Sci. Instrum. **70**, 525 (1999).
- **1.865 and 6.151 keV diagnostics successfully implemented on Z facility**
  - D.B. Sinars *et al.*, Rev. Sci. Instrum. **75**, 3672 (2004).

Photo of bent-crystal imaging hardware surrounding a wire array on Z

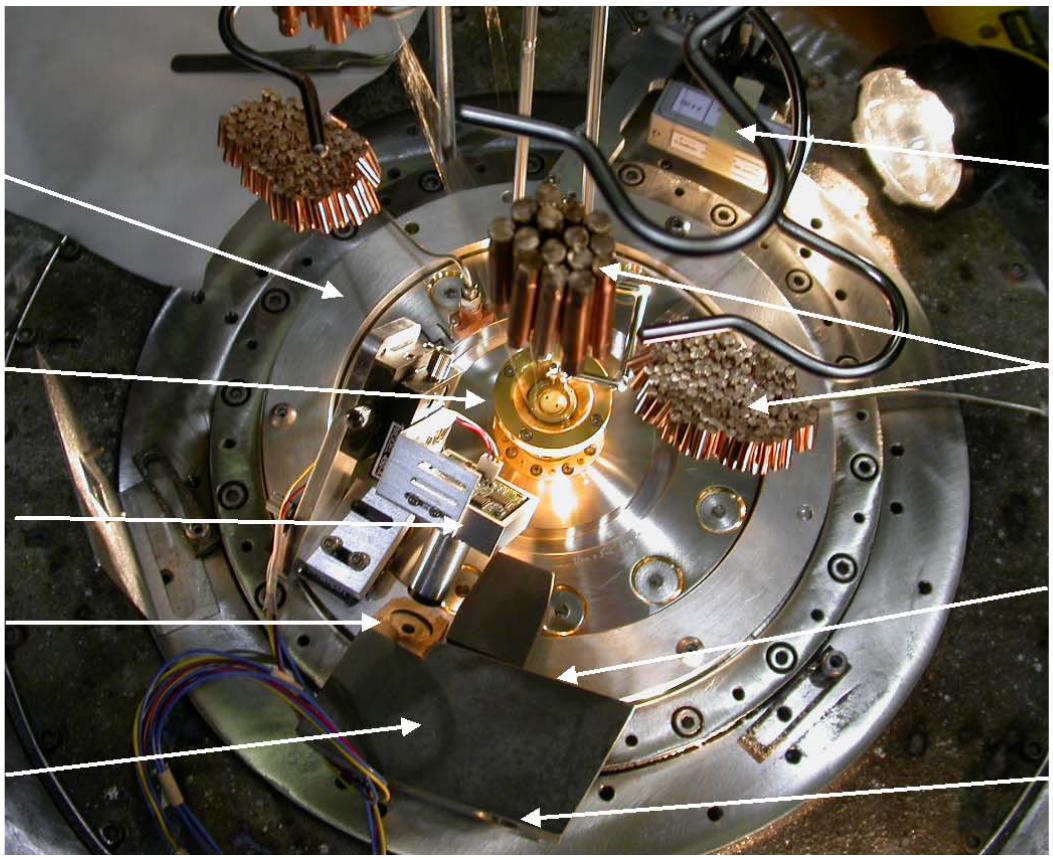

Most of this hardware is destroyed by the debris following the radiation burst

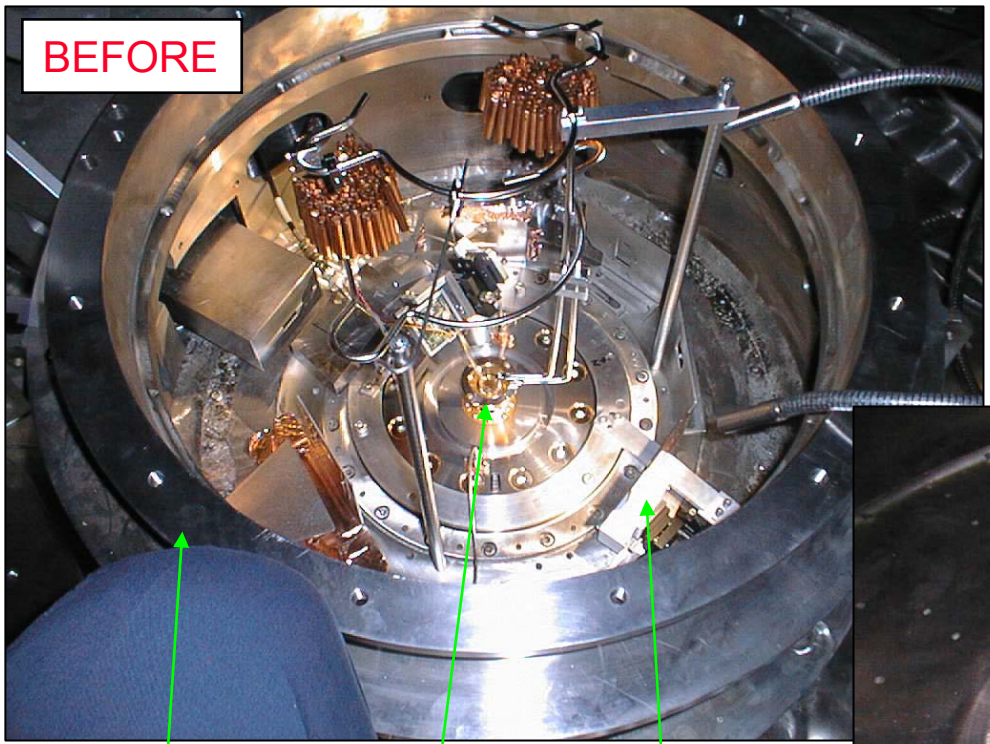

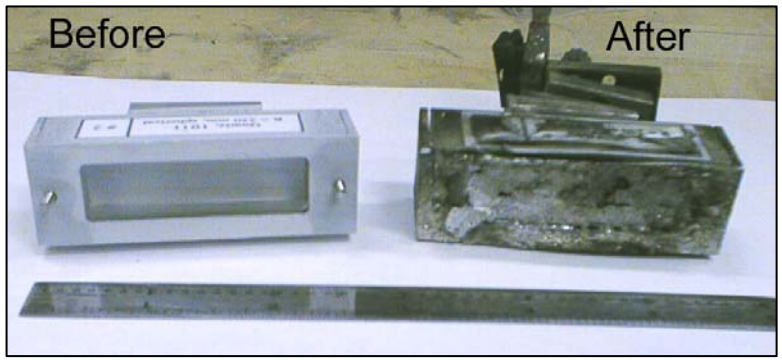

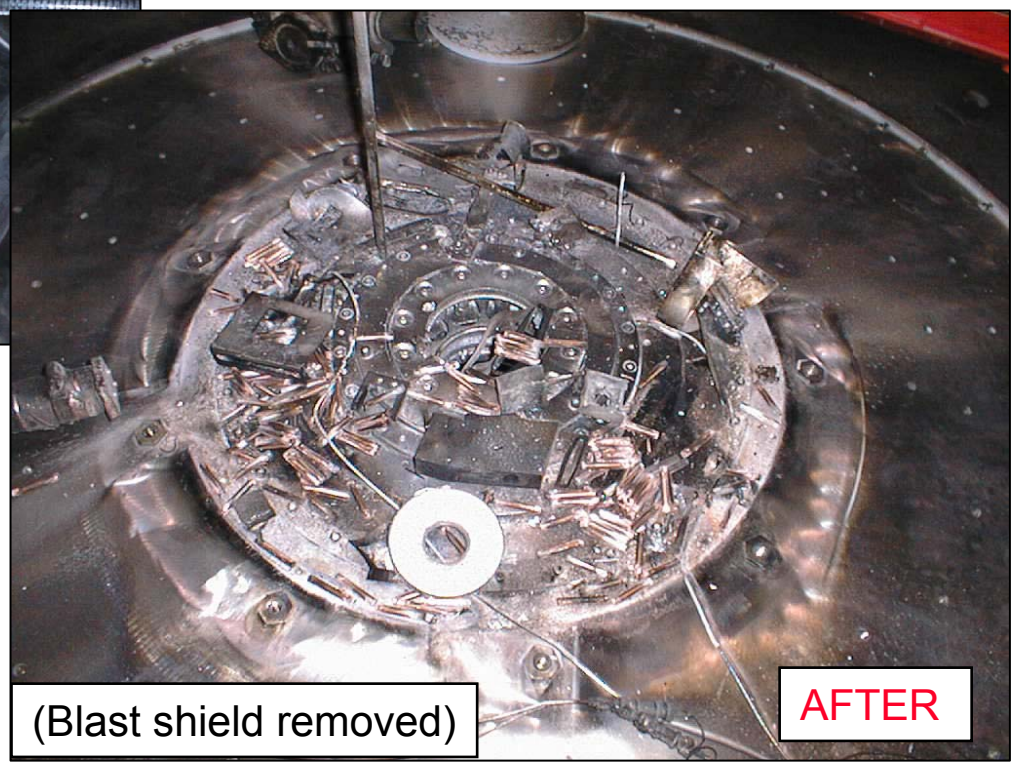

Energy release on Z equivalent to 1-2 sticks TNT

Single-sided-drive hemispherical capsule experiments* illustrate need for crystal imaging

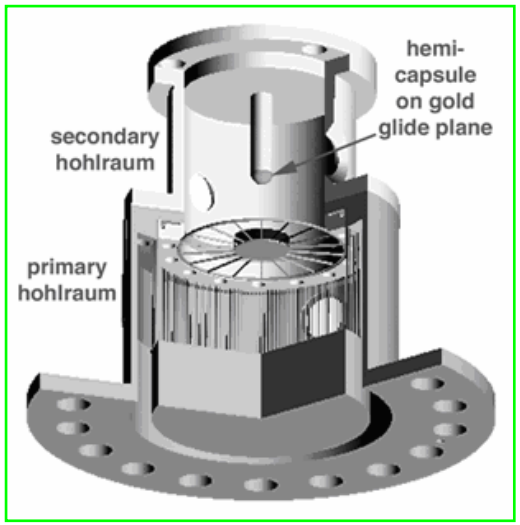

ϕ2.0mm, 60μm thk GDP hemi-shell on 30μm thk gold disc

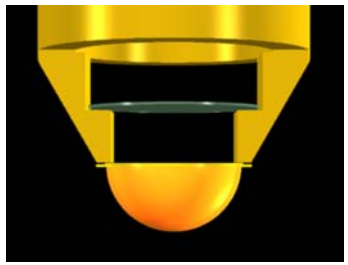

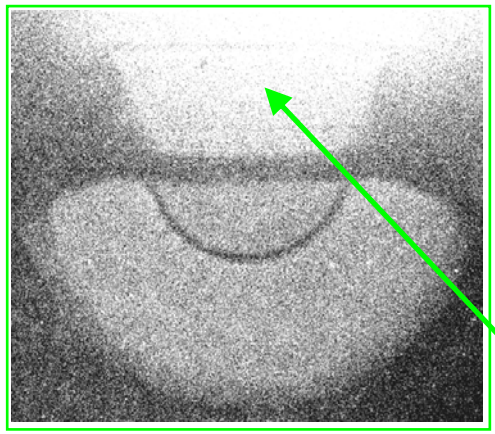

Point-projection radiography

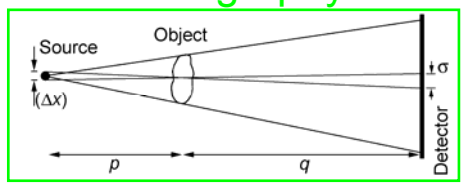

Background fog from z-pinch

Background fog necessitated a non-ideal geometry simply in order to get an image

Narrow spectral bandpass eliminated background, allowing optimal (shorter) secondary

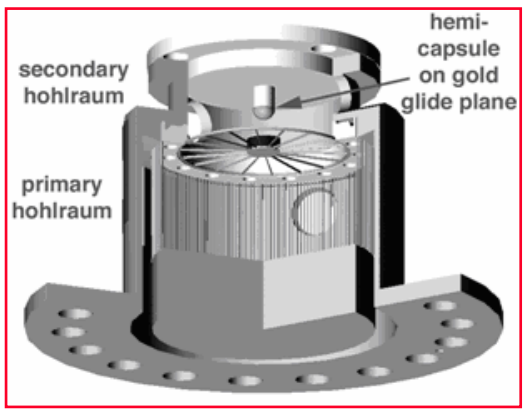

ϕ3.0mm, 110μm thk GDP hemi-shell on 8 deg glide plane

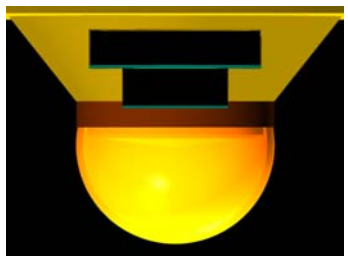

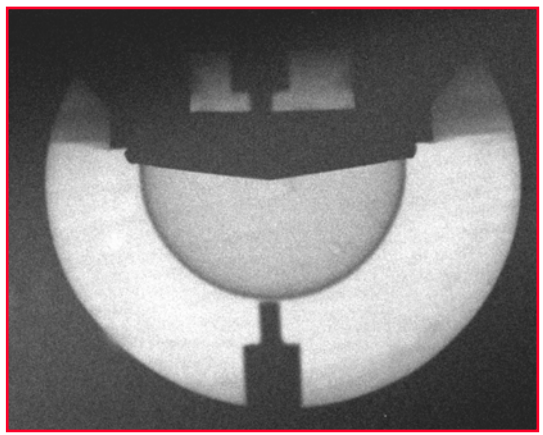

6.151 keV radiography

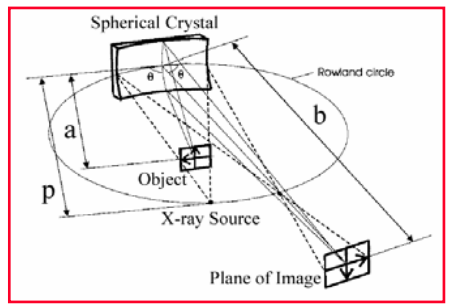

* D. L. Hanson *et al.*, Proc. IFSA 2003

The 6.151 keV backlighter has replaced the ~6.7 keV Fe system in ICF capsule tests*

3.4-mm diameter plastic ICF capsule

Capsules had 100s of known defects on surface that apparently produced a myriad of small jets

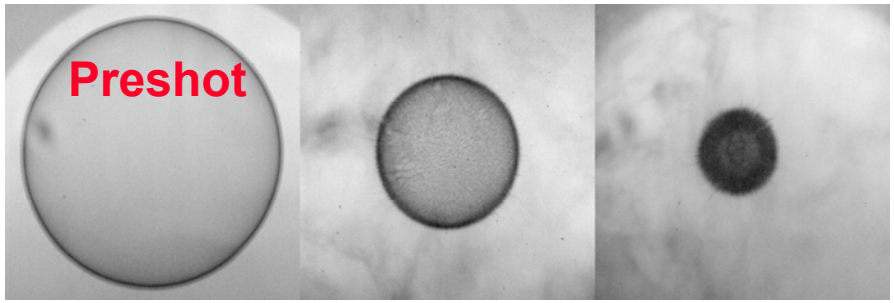

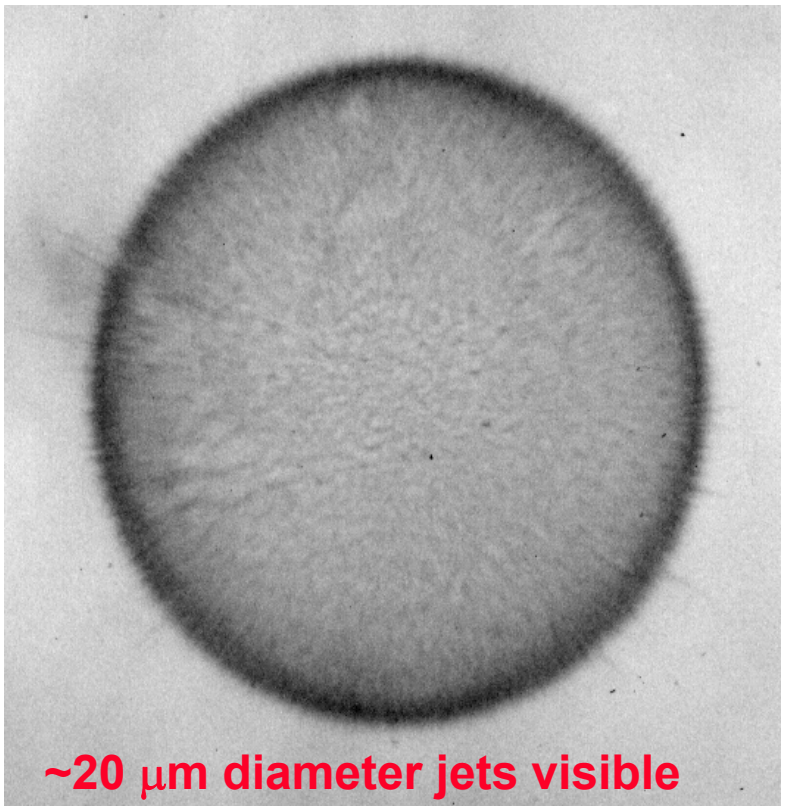

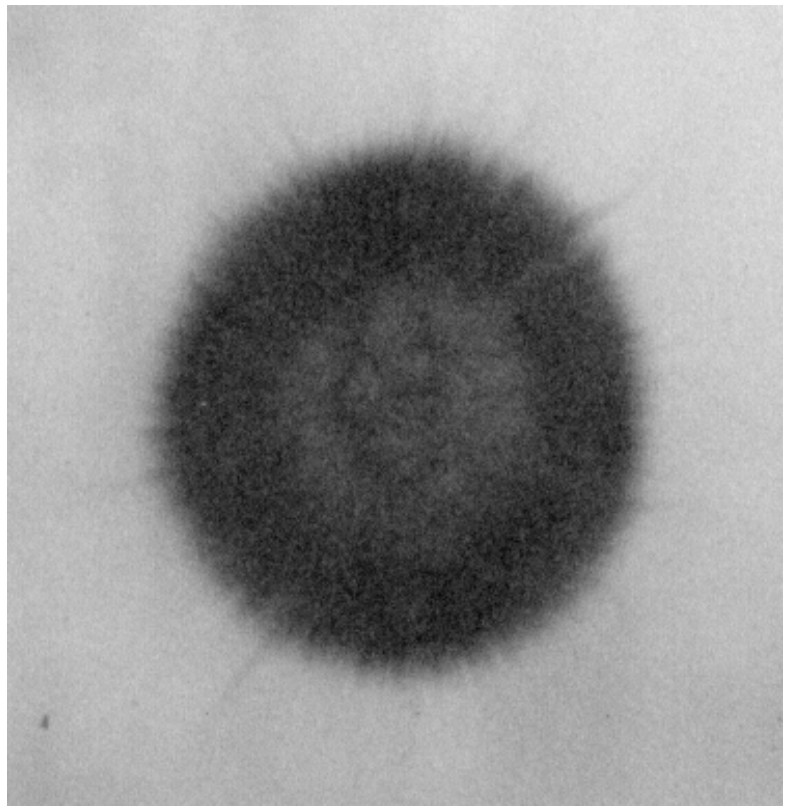

* M.E. Cuneo, G.R. Bennett

Placing the source inside the Rowland Circle can also boost the image intensity*

- **Moving the source inside the Rowland Circle:**
  - **Increases solid angle**
  - **Increase spectral bandpass**
- **Disadvantage is that the flat field starts to vary as the spectral shape gets convolved into it.**
- **This is useful for imaging small objects (<5 mm) and has been used in Radjet and ICF capsule tests**

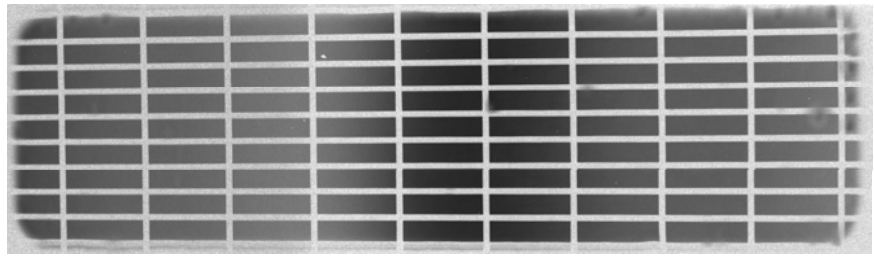

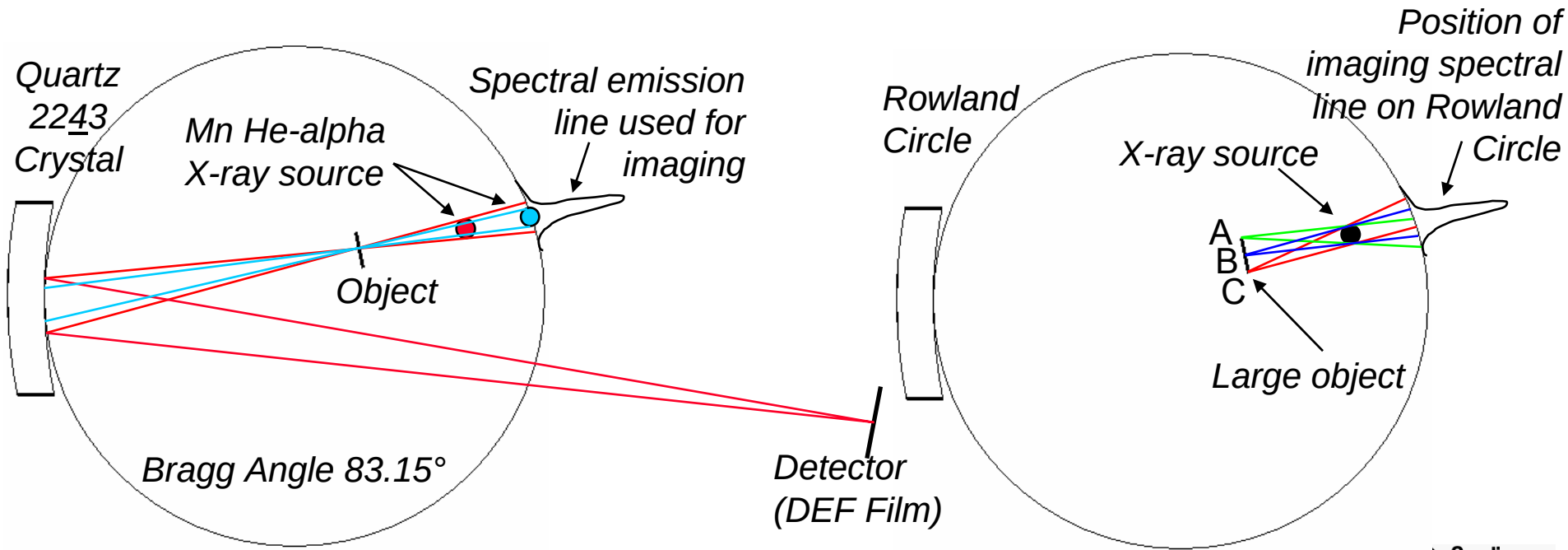

* D.B. Sinars *et al.*, Rev. Sci. Instrum. 75, 3672 (2004).
G.R. Bennett *et al.*, Rev. Sci. Instrum. 77, 10E322 (2006).

Work on advanced detectors at Sandia is ongoing

- **Imaging Plate (G.R. Bennett *et al.*)**
  - **Demonstrated to be 2-3x more sensitive than DEF film at 6.151 keV system on Z**
  - **Designed for >10 keV backlighters, so will scale well to Petawatt sources**
  - **Time-integrated**
  - **25-μm pixel size (resolution ~70 μm)**
  - **Investigating higher-resolution scanners**
- **Microchannel Plate (Ruggles *et al.*)**
  - **Proven technology, but making it a self-contained unit for vacuum chamber requires development work**
  - **Time-gated, eliminates self-emission from z-pinches, etc.**
- **Multiframe Ultrafast Digital X-ray Camera (G.R. Bennett *et al.*)**
  - **Fundamentally new detector being developed in collaboration w/ Sandia's MESA facility**
  - **4-8 frame *in-line* detector system**

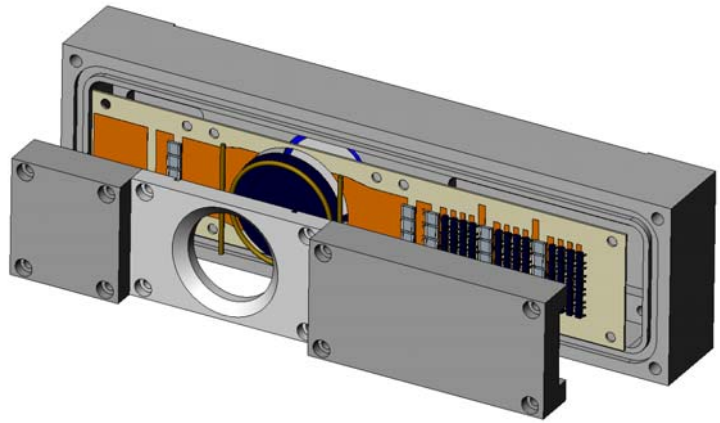

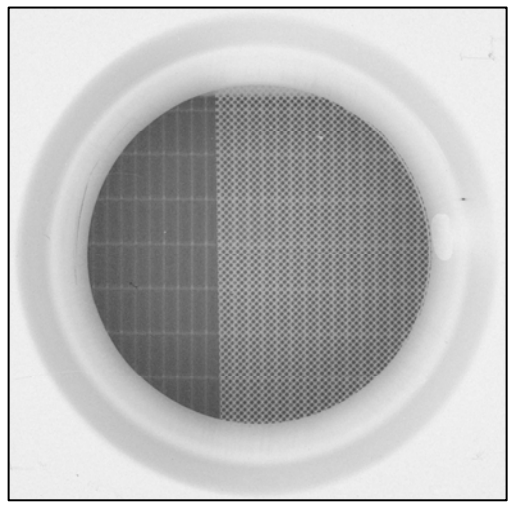

We briefly demonstrated 2-frame backlighting before the Z shutdown

Sandia National Laboratories

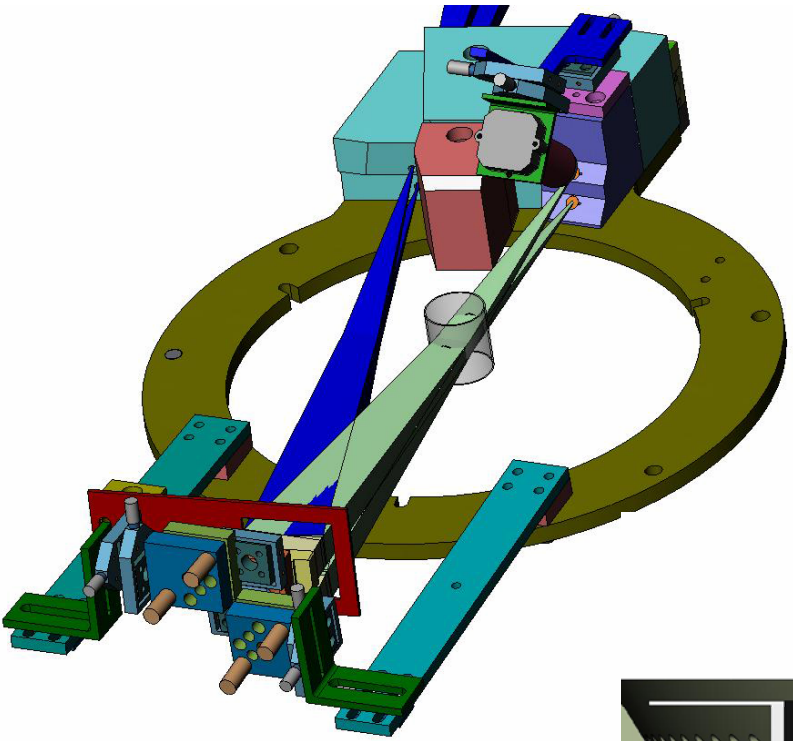

Z-Beamlet was modified to split the beam into two parts that focus in different places

Delays of 2 to ~20 ns between the two beams are possible.

System is designed to image a 4-mm-tall object with two 6.151 keV crystals

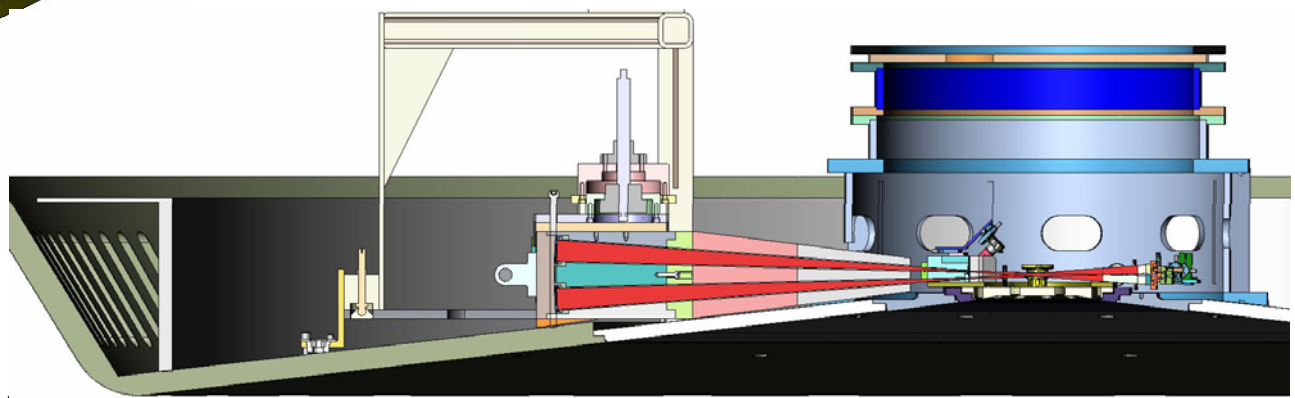

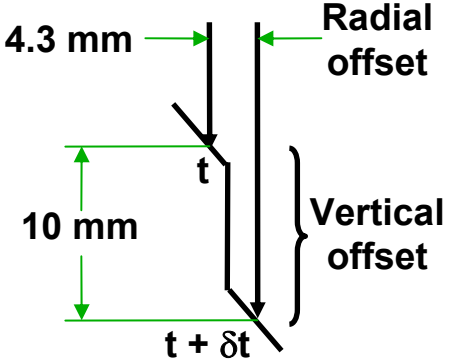

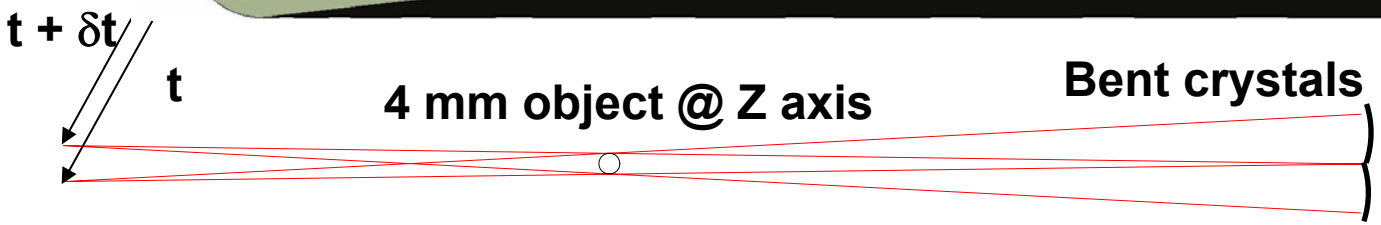

Why build a Petawatt Laser at Z?

- **Radiography in 10 < *hv* < 100 keV range**
  - **Z-pinch masses will nominally double in scaling from Z to ZR**
  - **~10 mg tungsten converged to a diameter of 2 mm:**
    T=0.000008% at 6.151 keV
    T=9% at 22 keV
- **Sub-picosecond image time resolution**
  - **Z-pinch implosion velocity ~0.5 mm/ns**
  - **For 1-ns ZBL pulse, ~0.5 mm blurring!**
  - **For 1-ps ZPW pulse, ~0.5 μm blurring**

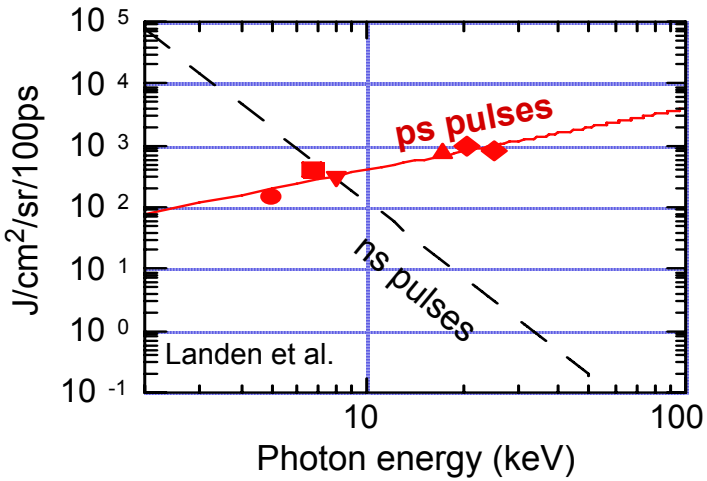

Kα conversion efficiency ~ 10^{-4} (Beg, Wharton, Park)

0.5kJ/0.5ps 1ω beam
→ 0.05 J of Kα emission
This is comparable to time-integrated energy >15 keV from z pinches on Z

Sandia National Laboratories

Z-Petawatt Project

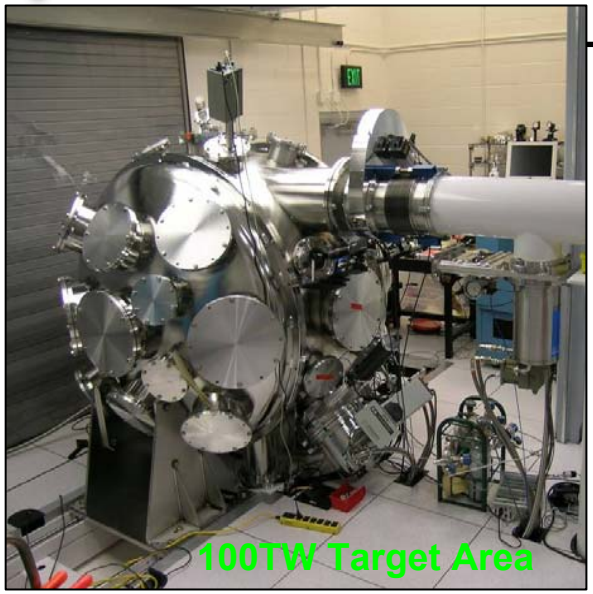

FY06 ~100 TW

≤ 50 J, 0.5 - 10 psec
- Bldg 983 remodel completion
- Main amplifier activation (finished)
- Sub-aperture compression and target testing (started)

FY07 ~1000 TW

≤ 500 J, 0.5 - 10 psec
- Beam transport to Z activation
- Full-Aperture Grating Compressor activation
- All-reflective FOA activation
- Radiography diagnostics fielded on ZR

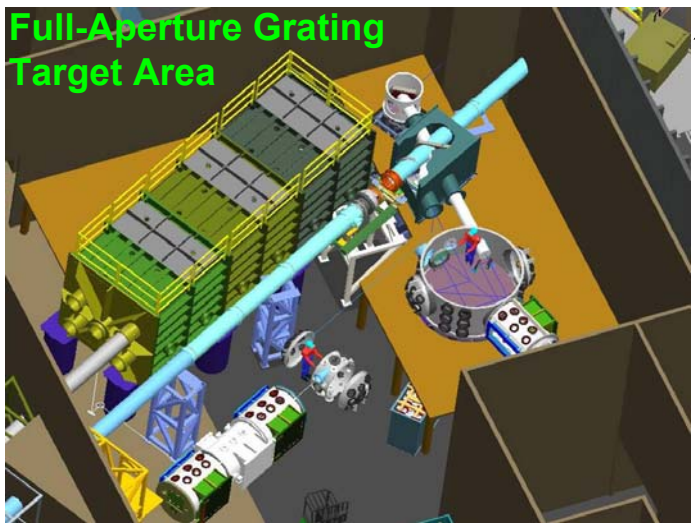

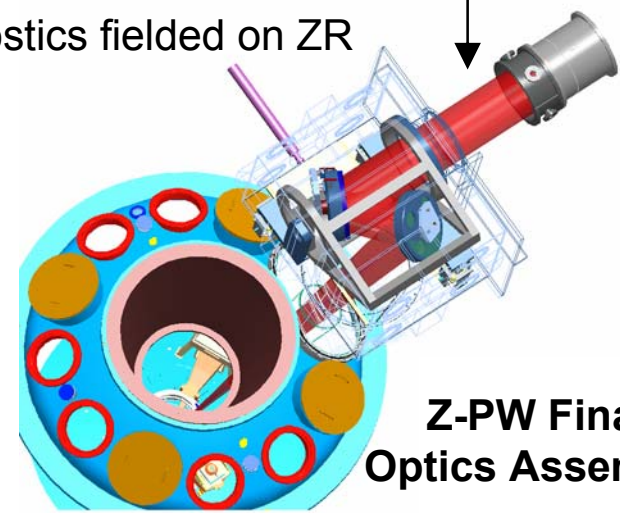

Z-PW Final Optics Assembly

Table of Contents

Sandia National Laboratories

Useful web sites for x-ray absorption and scattering calculations

X-ray interactions with matter
http://henke.lbl.gov/optical_constants/

NIST Scientific and Technical Databases
http://www.nist.gov/srd/physics.htm

XCOM Database:
A web database which can be used to calculate photon cross sections for scattering, photoelectric absorption and pair production, as well as total attenuation coefficients, for any element, compound or mixture (Z=1-100), at energies from 1 keV to 100 GeV.
http://physics.nist.gov/PhysRefData/Xcom/Text/XCOM.html

Theoretical Form Factor, Attenuation, and Scattering Tabulation for Z = 1-92 from E = (1-10 eV) to (0.4-1.0 MeV)
http://physics.nist.gov/PhysRefData/FFast/Text/cover.html

Selected Radiography Publications from Z/ZBL

- **Point-projection Backlighting Diagnostics**
  - G.R. Bennett *et al.*, Rev. Sci. Instrum. 72, 657 (2001).
  - L.E. Ruggles *et al.*, Rev. Sci. Instrum. 74, 2206 (2003).
- **Point-projection ICF Capsule Experiments**
  - G.R. Bennett *et al.*, Phys. Rev. Lett. 89, 245002 (2002).
  - R.A. Vesey *et al.*, Phys. Rev. Lett. 90, 035005 (2003).
  - G.R. Bennett *et al.*, Phys. Plasmas 10, 3717 (2003).
  - R.A. Vesey *et al.*, Phys. Plasmas 10, 1854 (2003).
- **Crystal Imaging Backlighting Diagnostics**
  - D.B. Sinars *et al.*, Appl. Optics 42, 4059 (2003).
  - D.B. Sinars *et al.*, Rev. Sci. Instrum. 75, 3672 (2004).
- **Wire-array Z-pinches (Crystal Imaging)**
  - D.B. Sinars *et al.*, Phys. Rev. Lett. 93, 145002 (2004).
  - D.B. Sinars *et al.*, Phys. Plasmas 12, 056503 (2005).
  - M.E. Cuneo *et al.*, Phys. Rev. Lett. 94, 225003 (2005).
  - M.E. Cuneo *et al.*, Plasma Phys. Contr. Fusion 48, R1 (2006).
  - D.B. Sinars *et al.*, Phys. Plasmas 13, 042704 (2006).
  - M.E. Cuneo *et al.*, Phys. Plasmas 13, 056318 (2006).
- **Radiation-driven Jet/Capsule Experiments (Crystal Imaging)**
  - G.R. Bennett *et al.*, Rev. Sci. Instrum. 77, 10E322 (2006).
  - G.R. Bennett *et al.*, (submitted to Phys. Rev. Lett., 2007).
- **LANL Blastwave Experiments (Crystal Imaging)**
  - R. Peterson *et al.*, Phys. Plasmas, (in press, 2006).